NASA CONTRACTOR REPORT

RESEARCH AND DEVELOPMENT OF A SINGLE GUN COLOR CRT

Phase II - Final Report

by Thomas E. Sisneros, Paul A. Faeth, and Joseph A. Davis

Prepared by
ITT ELECTRON TUBE DIVISION
Fort Wayne, Ind.
for Electronics Research Center

NATIONAL AERONAUTICS AND SPACE ADMINISTRATION • WASHINGTON, D. C. • FEBRUARY 1970

RESEARCH AND DEVELOPMENT

OF A SINGLE GUN COLOR CRT

Phase II - Final Report

By Thomas E. Sisneros, Paul A. Faeth, and Jospeh A. Davis

Prepared under Contract No. NAS 12-534 by
ITT ELECTRON TUBE DIVISION
Fort Wayne, Ind.

for Electronics Research Center

NATIONAL AERONAUTICS AND SPACE ADMINISTRATION

For sale by the Clearinghouse for Federal Scientific and Technical Information
Springfield, Virginia 22151 – Price $3.00

TABLE OF CONTENTS

LIST OF ILLUSTRATIONS

PHASE II FINAL REPORT
RESEARCH AND DEVELOPMENT
OF A
SINGLE GUN COLOR CRT

By Thomas E. Sisneros, Paul A. Faeth and Joseph A. Davis

ITT Electron Tube Division
Fort Wayne, Indiana

SUMMARY

The factors influencing superlinear phosphor behavior have been investigated, and the final results presented herein.

The more important phosphor synthesis parameters were investigated in this continuation of the study of the factors responsible for superlinear and sublinear cathodo luminescence.

Phosphors with pronounced superlinear and sublinear character have been synthesized, and the better phosphors employed in the fabrication of 5-inch CRT's. Color gamuts covering the range of colors from greenish-yellow to orange-red have been obtained with beam current densities of 0.05 to 10 $\mu a/cm^2$.

Relative brightness of the final quarterly tube, Q-2, ranged from 0.9 ft lamberts at 0.05 $\mu a/cm^2$ beam current density to 400 ft lamberts at 10.0 $\mu a/cm^2$ and 15 kv beam voltage.

INTRODUCTION

This report describes the studies and results of Phase II on the research and development of a single gun color CRT. The Phase I final report was published as NASA Contract Report CR-1228 December, 1968. The investigations conducted and reported herein include the objectives set forth in the contract extension proposal as follows:

a. The effect on superlinearity of variations in preparative conditions, for (Zn, Cd)S:Ag:Ni compositions which yield red and green luminescence. The variations include:

   1. The effect of different compounds as fluxes.

   2. The influence of gas atmospheres on the high temperature recrystallization process.

   3. Separate incorporation of Ag and Ni.

   4. Effect of recrystallization time and temperature.

b. The effect of nickel on the luminescence of lanthanide activated sulfides.

c. The preparation and evaluation of linear and sublinear phosphors with green luminescence for use with superlinear red phosphors.

d. The preparation and evaluation of linear and sublinear phosphors with red luminescence for use with green emitting superlinear phosphors.

e. The investigation of phosphors with an emission color other than red or green, for use in preparing mixtures of a linear or sublinear phosphor with a superlinear phosphor. The investigation includes phosphors for mixtures which produce red-blue or red-blue green color shifts with changing current density.

f. Studies designed to elucidate the mechanism of superlinear and sublinear luminescence.

g. The preparation and evaluation of phosphors containing lanthanide activators for their ability to shift luminescence color as a function of excitation intensity.

h. The study of ultraviolet luminescent materials for superlinear behavior.

i. The evaluation of screens of phosphor mixtures for use in CRTs.

TECHNICAL DISCUSSION

Phosphor Synthesis and Evaluation

The general procedures employed in the synthesis, measurement, and evaluation of phosphors and the principles of superlinear and sublinear phosphor behavior were described in the Phase I report (CR 1228). In this report phosphor evaluation was performed employing settled screens of the phosphors, unless specifically designated otherwise. A detailed discussion is given in Section 2. 9 of the technical discussion.

In all the figures illustrating phosphor output intensity as a function of beam current density, the numerical values represent the output signal in microamperes of a 1P21 photomultiplier with a Wratten 106 filter. This photomultiplier-filter combination closely approximates the response of the normal photopic eye.

The output of the photomultiplier with Wratten filter has been adjusted to read 10. 0 μa for a standard P-1 phosphor at a beam current density of 0. 5 $\mu a/cm^2$ for powders and 1. 0 $\mu a/cm^2$ for screens.

The use of this reference setting permits the comparison of all data represented on the figures.

The Influence of Flux Compound Type and Firing Time and Temperature on Luminescence Intensity and Superlinear Behavior

The effect of flux compounds on the intensity of luminescence and the powder physical characteristics of phosphors is well known Some work with different flux compounds was reported near the end of Phase I, and it was decided to undertake a more extensive evaluation of the influence of flux compounds on the established superlinear sulfide compositions. Most of the previous effort was conducted employing NaCℓ as the flux compound. The use of sodium chloride as a flux produced a considerable sintering and particle aggregation. Furthermore, sulfide phosphors consisting of high percentages of cadmium sulfide sinter at relatively low temperatures and produce phosphor samples that are difficult to apply in phosphor screen fabrication. Grinding is frequently required, but is not recommended when maximum luminescence intensity is desired. The study of flux compound effects on particle (or aggregate) size and phosphor brightness was made previously as part of a company supported project. In this study bromide compounds were shown to function as efficient fluxes in ZnS and (Zn, Cd)S phosphors. A variety of bromide compound fluxes were used in the synthesis of superlinear green and red phosphors. The most successful fluxes were KBr, and KBr + $BaBr_2$. The effect on superlinear behavior compared to the best superlinear phosphors prepared is shown in Figures 1 and 2 for green and red phosphor screens. The data on these and other samples are reported in the Appendices. The phosphor screen composition for data reported in Appendix B is found in Appendix A.

The use of bromide fluxes in the preparation of superlinear green phosphor produced a significant shift in chromaticity coordinates relative to sodium chloride fluxed samples. This chromaticity shift indicated that the spectral energy distribution (SED) curve for the phosphor is shifted toward longer wavelengths and requires a composition variation to correct the chromaticity of the green superlinear phosphor to correspond to the reference phosphor composition.

The effect of bromide fluxes on the chromaticity of the superlinear red phosphors was negligible The same SED is obtained for red phosphors, with a high Cd/Zn ratio, regardless of the flux type employed during synthesis.

Calcium chloride was also employed as a flux for both green and red superlinear phosphor synthesis. This compound was chosen because it is widely used in the preparation of P-20 type phosphors, and other yellow-emitting phosphors used in P-4 phosphor preparations. However, $CaCℓ_2$ produces extensive sintering in the firing process, and is therefore difficult to handle in screen preparation. Similar superlinear behavior to NaCl fluxed samples results from the use of $CaCℓ_2$, as shown in Figures 1 and 2.

An attempt to resolve the uncertainty regarding the concentration of nickel actually present in the superlinear phosphor compositions was made employing sodium fluoride as the flux compound in the prefiring step. Fluorides are known to produce rapid crystal growth in sulfide phosphors, presumably through increased solubility of sulfides in fluoride melts. Therefore, nickel should be incorporated into the host

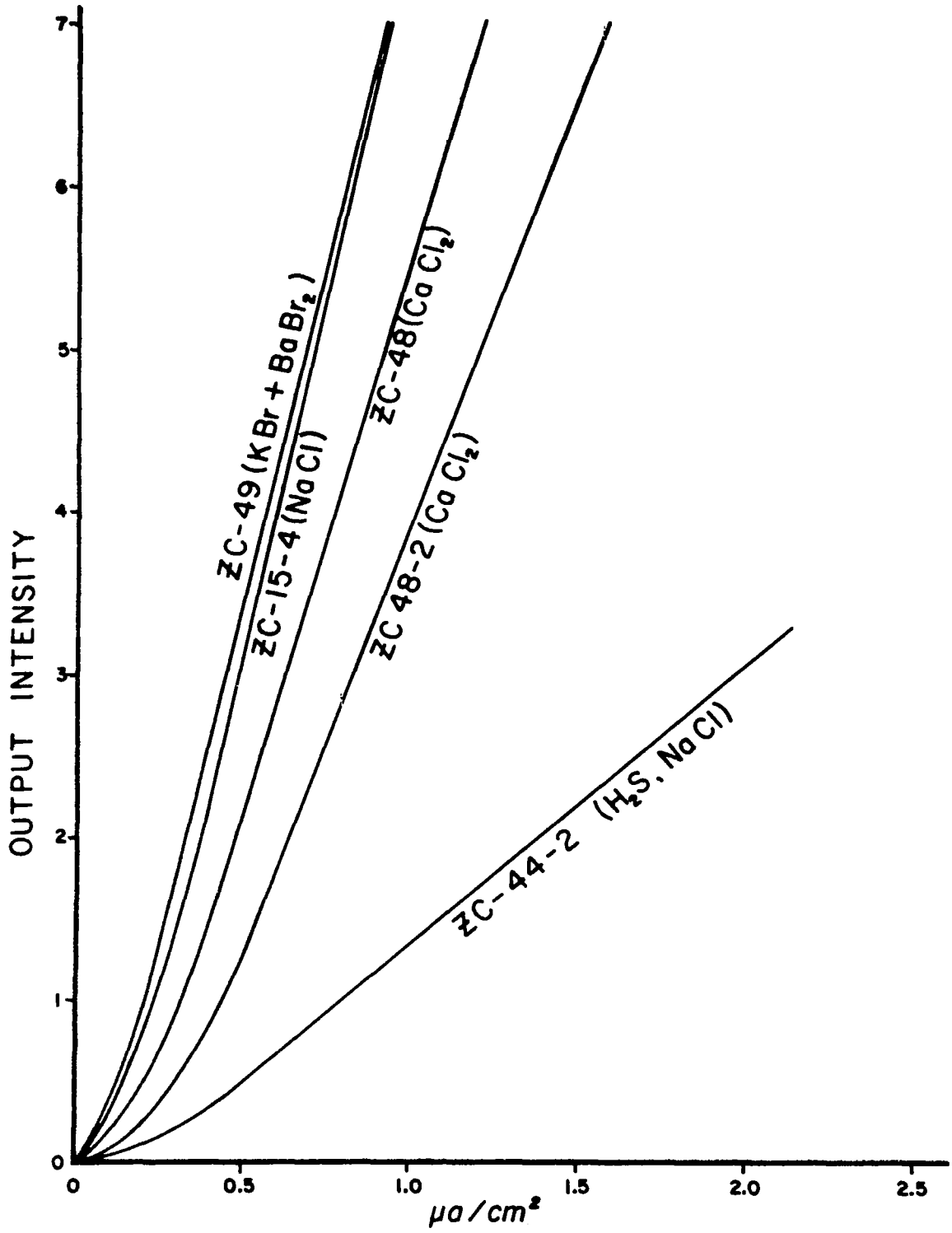

Figure 1. Intensity Versus Current Density (Screen Data)

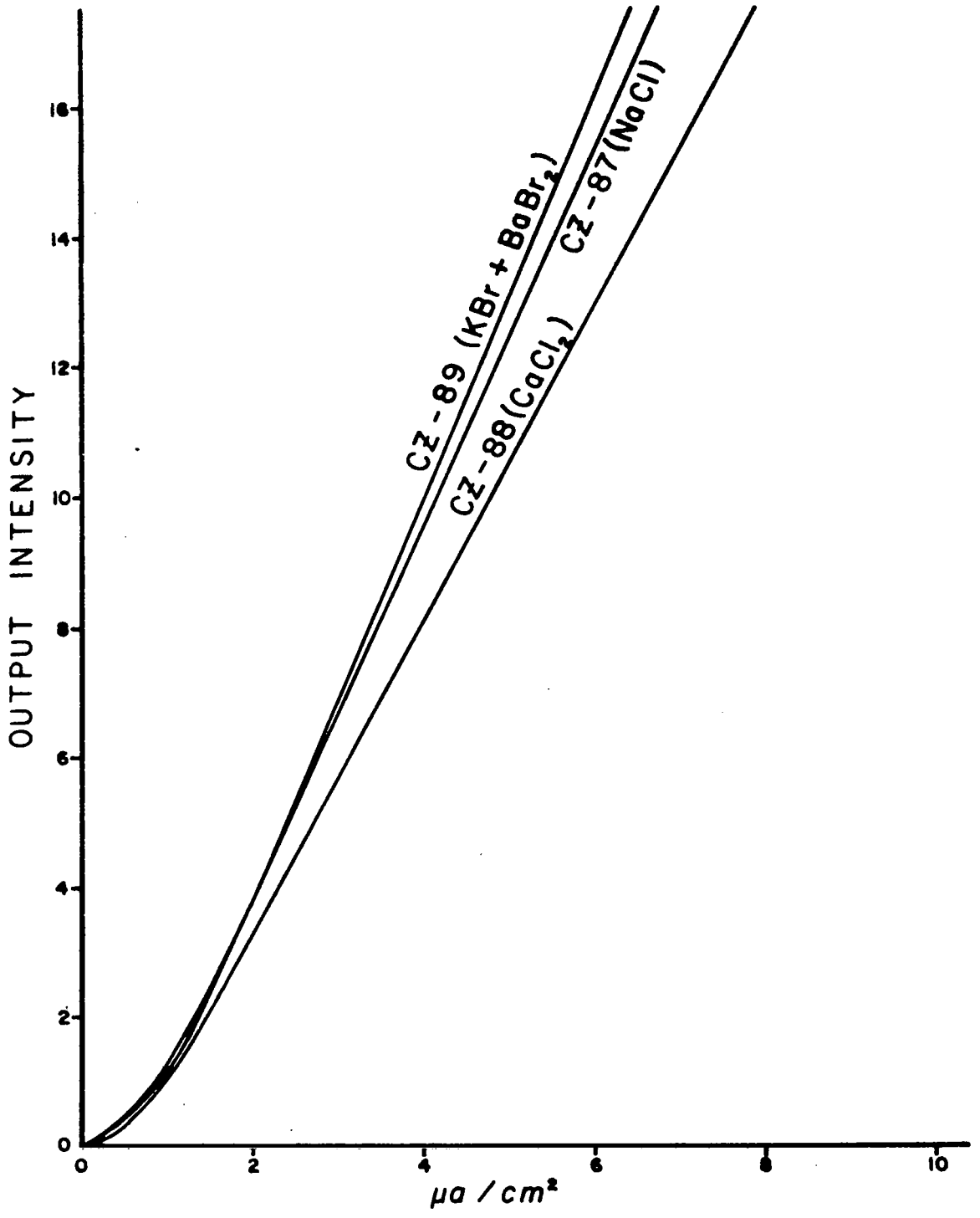

Figure 2A. Intensity Versus Current Density (Screen Data)

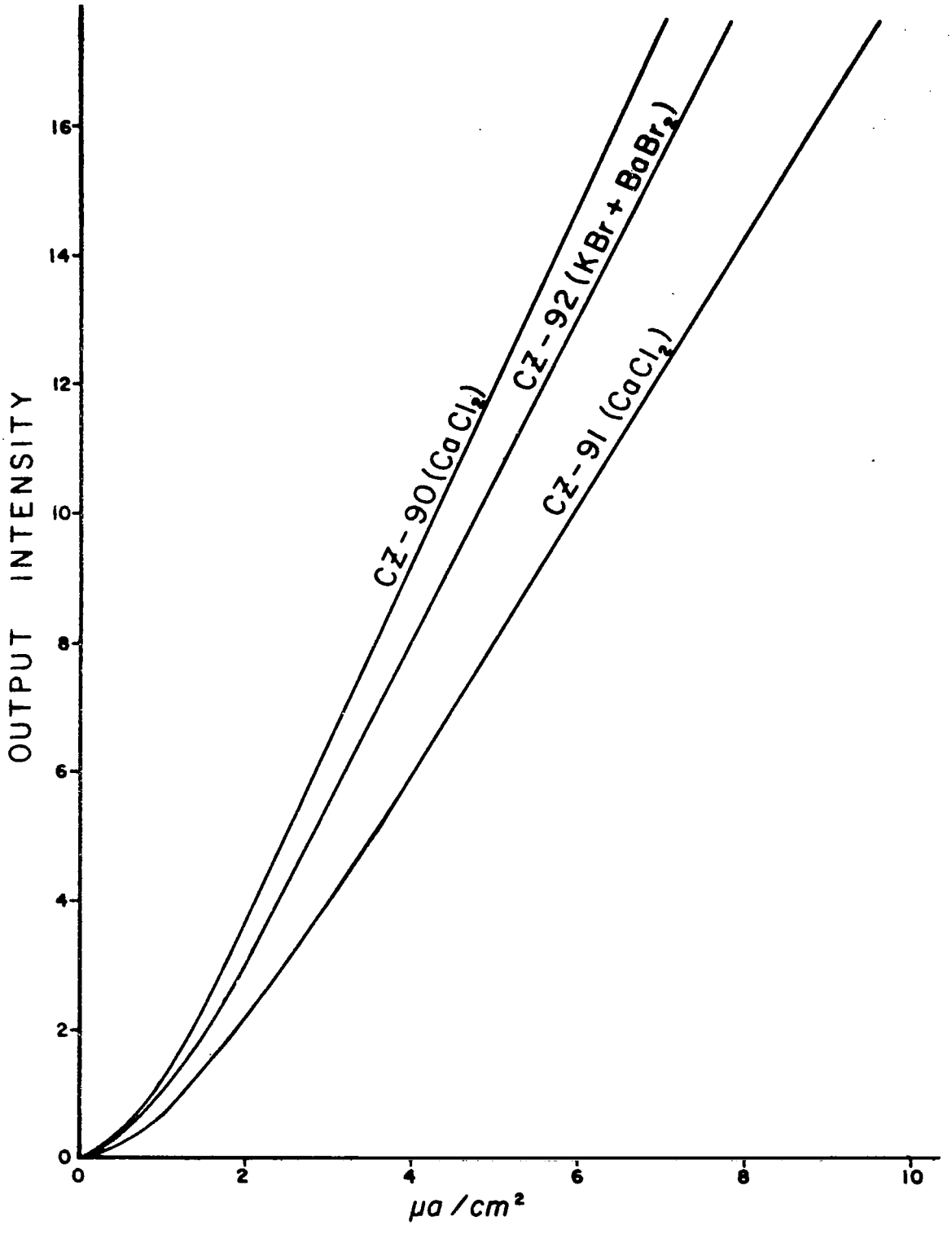

Figure 2B. Intensity Versus Current Density (Screen Data)

lattice more efficiently. A second firing with the normal NaCl flux and Ag activator was then performed to obtain a luminescent material. Experimental samples were prepared with nickel concentrations of 2, 4, and 8 ppm Ni at several prefiring temperatures (750° and 850°C) and refired with NaCl flux and 50 ppm Ag, employing a 50/50 ratio of ZnS/CdS. All of the samples exhibited reduced output intensity and poor superlinearity. The data are reported in Appendix A. The characteristics of these and other green superlinear powder phosphors should be compared to a "standard" superlinear phosphor, sample, ZC-15-4 also shown in Appendix A. Note that the output intensity is higher for samples prepared at lower (650°C) temperatures and the superlinearity is greatest for the higher (8 ppm) nickel concentration. Because fluorides did not improve superlinearity or brightness and in fact supported the earlier finding that 7.5 ppm Ni produced the optimum superlinear behavior, further work with this flux was discontinued.

In addition to the use of calcium chloride and the bromide flux compounds in the preparation of red emitting sulfides, both $ZnCl_2$ and $CdCl_2$ were employed (see Figure 3). The effect of firing time and temperature was also determined using $CaCl_2$ flux (samples CZ87 through 92, Figure 2). A series of double firing studies were performed with the red sulfide composition and the fluxes mentioned above (powder data on CZ82-86 is in Figure 3).

Firing Atmosphere Effects

The use of gas atmospheres in place of flux compounds in the high temperature synthesis of phosphors frequently produces improved brightness characteristics. The improvement is usually attributed to a more complete activator and co-activator incorporation in the host crystal phosphors. For sulfide phosphor synthesis, hydrogen sulfide has been used to introduce activator and coactivator elements, presumably through the formation of sulfides of the elements. In some phosphors, the incorporation of activator elements is not accomplished unless H_2S is used. The lanthanide activator elements will function as efficient activators in sulfides only when H_2S atmosphere firing is used.

Samples of red (Zn, Cd)S:Ag:Ni phosphor (CZ76-9) prefired in H_2S with Ni present in the prefiring step, produced phosphors with a somewhat poorer superlinearity than the best superlinear red phosphor at firing temperatures below 850°C.

The optimum firing conditions were found to be a temperature of 850°C for both the first and second firing steps for three hours each. Intensity ratios(*) of about 55 were obtained, which are nearly equivalent to the best superlinear red phosphor previously prepared (i.e. CZ61-7 had an intensity ratio of 65). Sample CZ61-11, illustrated in Figure 4, is much improved over the earlier sample.

---

* The "Intensity ratio" is an arbitrary means for evaluating the extent of superlinearity in a phosphor, as defined in the Phase I report. The intensity of 1.0 $\mu a/cm^2$ is divided by the intensity at 0.05 $\mu a/cm^2$. A perfectly linear phosphor would have an intensity ratio of 20.

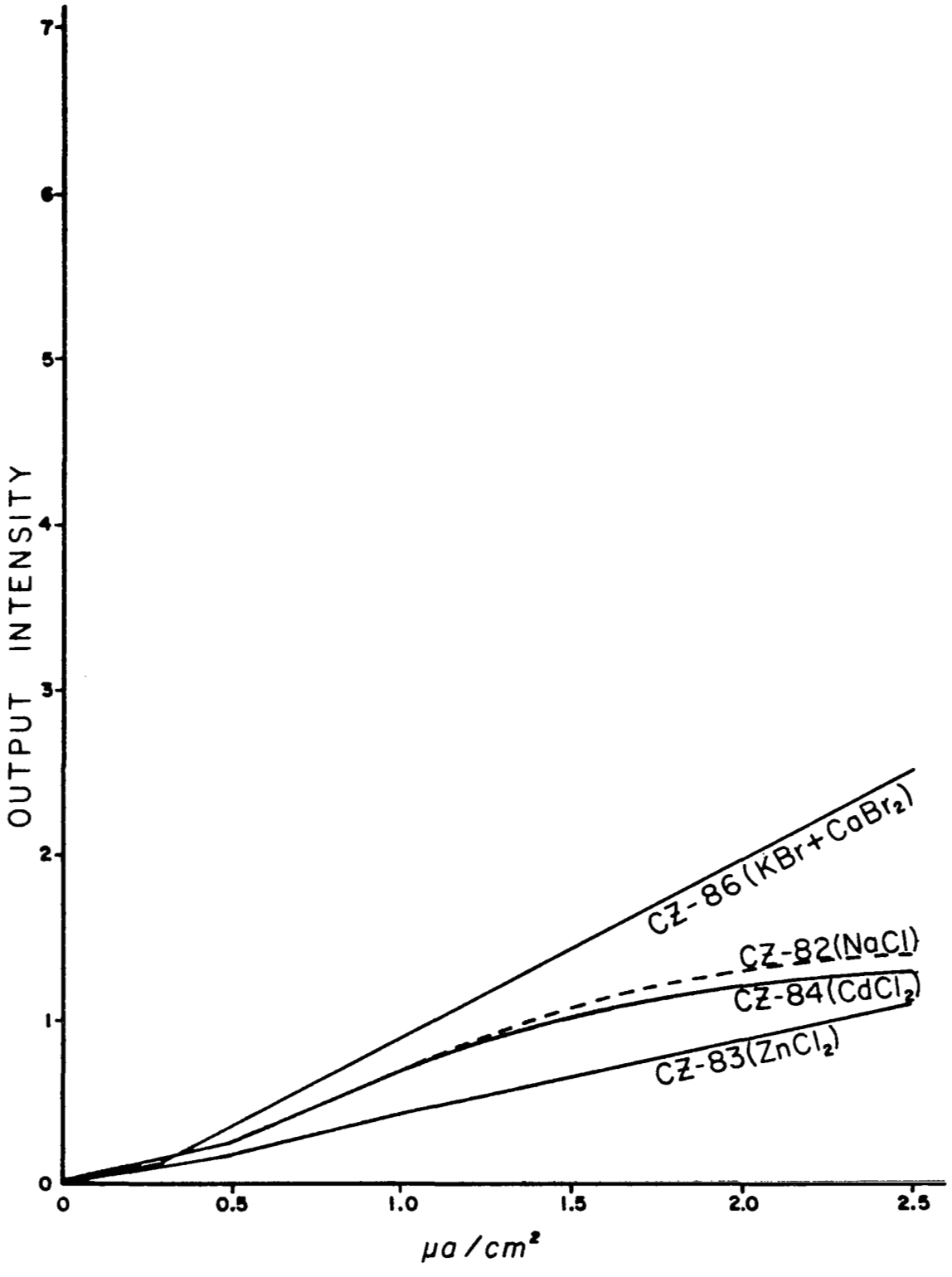

Figure 3. Intensity Versus Current Density (Powder Data)

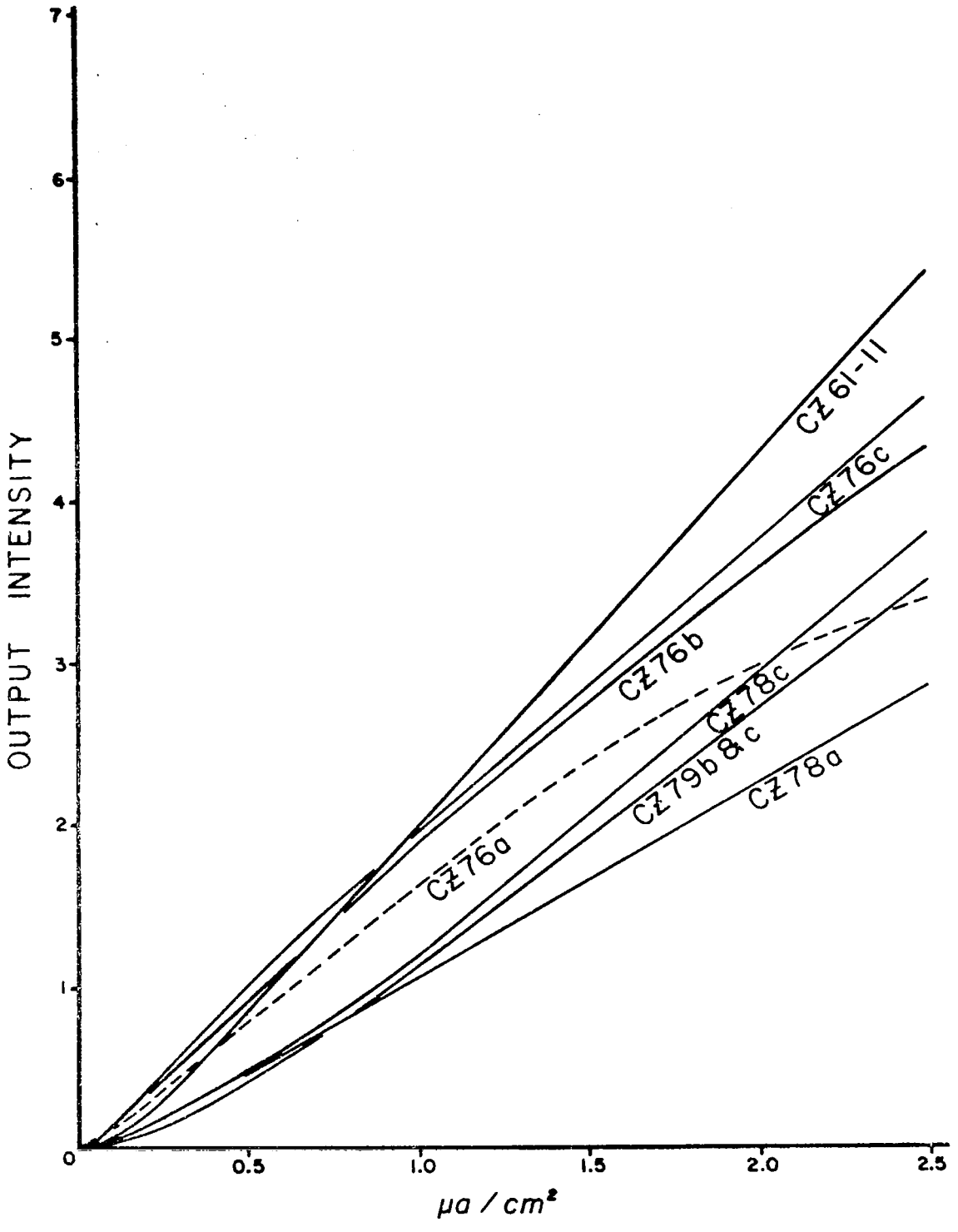

Figure 4. Intensity Versus Current Density (Powder Data)

The procedure applied to the incorporation of nickel in (Zn, Cd)S was prefiring the raw material in H_2S at 750°C, 850°C, and 950°C. A second firing using the normal NaCl flux treatment for introducing the silver activator followed the H_2S prefiring step. The phosphor screen evaluation of output intensity versus current density is shown in Figure 4 and the data reported in Appendices A and B. From Figure 4 it can be seen that while superlinear behavior is reasonably good, no significant improvement over the conventional flux methods of nickel incorporation is obtained.

The use of H_2S atmosphere firing in the preparation of green sulfides with several other fluxes including $CaCl_2$ were employed in the second firing stage. None of the samples exhibited improved superlinearity. (See Appendix A and Figure 5A.) The comparison of screen and powder behavior is also shown in Figure 5B.

Nickel Concentration and Incorporation Methods

A series of superlinear green phosphor employing $CaCl_2$ as the flux was prepared in which the silver-nickel concentration was varied. The optimum nickel and silver concentrations obtained were essentially the same as those employed in samples prepared with sodium chloride flux. The plots of intensity versus current density for screens are given in Figure 6 and the data is reported in Appendices A and B for powder and screen, respectively.

Note that the intensity ratio for 7.5 ppm Ni + 50 ppm Ag in sample ZC48-2 is 88, while for ZC52 and 54 the intensity ratio is 124 and 120 respectively.

The problem of assurance that complete incorporation of Ni occurs was approached from still another point, namely, to coprecipitate nickel and zinc sulfide and use the resulting stock mixture as the source of Ni. Concern with the normal method of addition stems from the possibility that locally high concentrations of NiS may result when a solution containing the nickel is added to a stirred ZnS or a mixture of ZnS and CdS.

Several stock mixtures of NiS and ZnS were made and used to prepare (Zn, Cd)S:Ag green and red phosphor compositions. (See sample CZG-4, 5, 6 and ZCE-4, 5, 6 in Appendix A.) The analysis of the data revealed that little or no superlinearity resulted. An explanation can only come from assuming that the prior coprecipitation actually immobilized the Ni in the phosphor mixture. Therefore, it must be concluded that the solution method actually provides the most uniform distribution of Ni in the fired phosphor.

Sample Reproducibility

Sample reproducibility was also investigated, because in the past, identical samples exhibited widely varying superlinear character. The more recent studies of reproducibility have not shown this variation and it is now felt that successive, identical, sample preparations can be accomplished (see Appendices A and B).

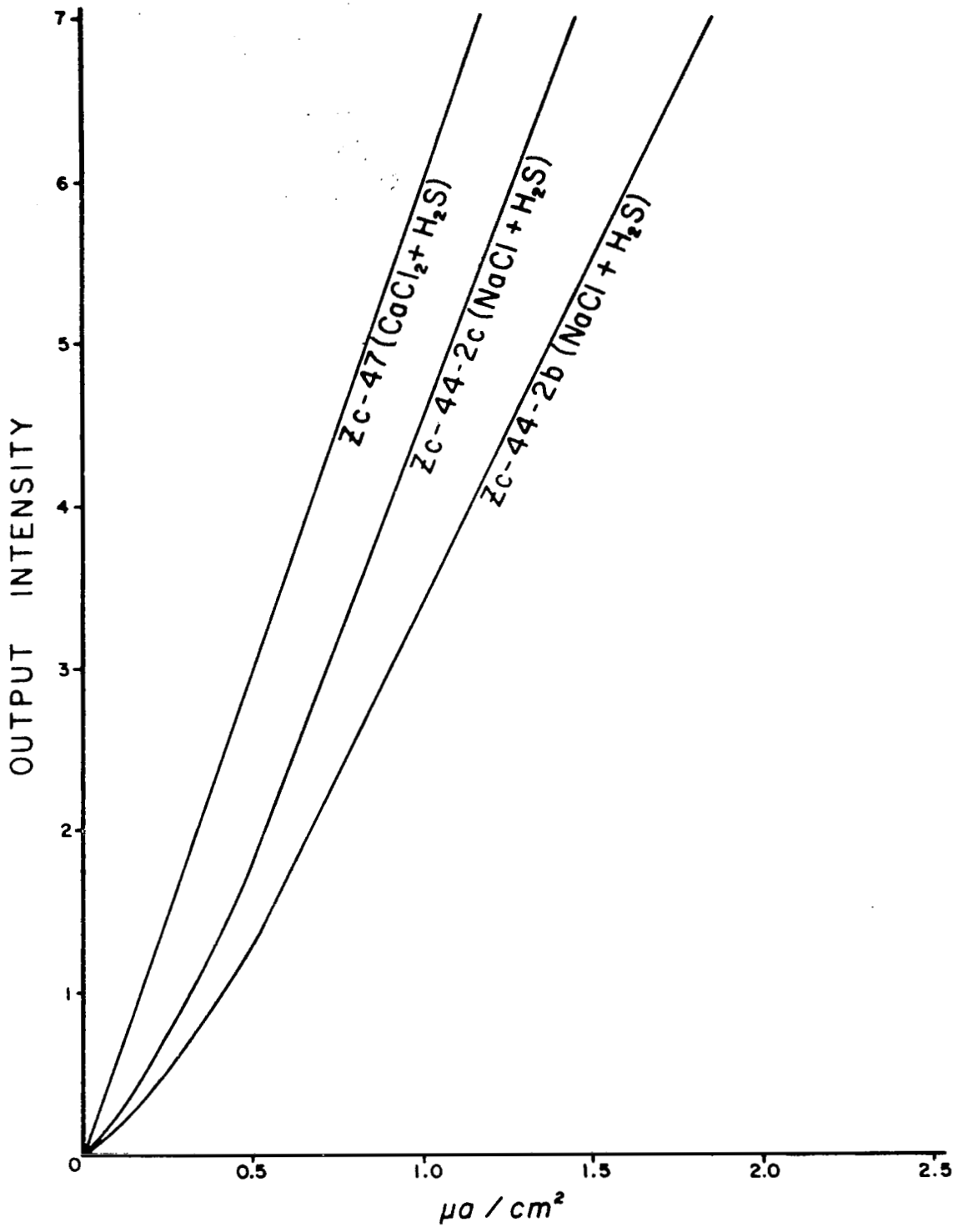

Figure 5A. Intensity Versus Current Density (Powder Data)

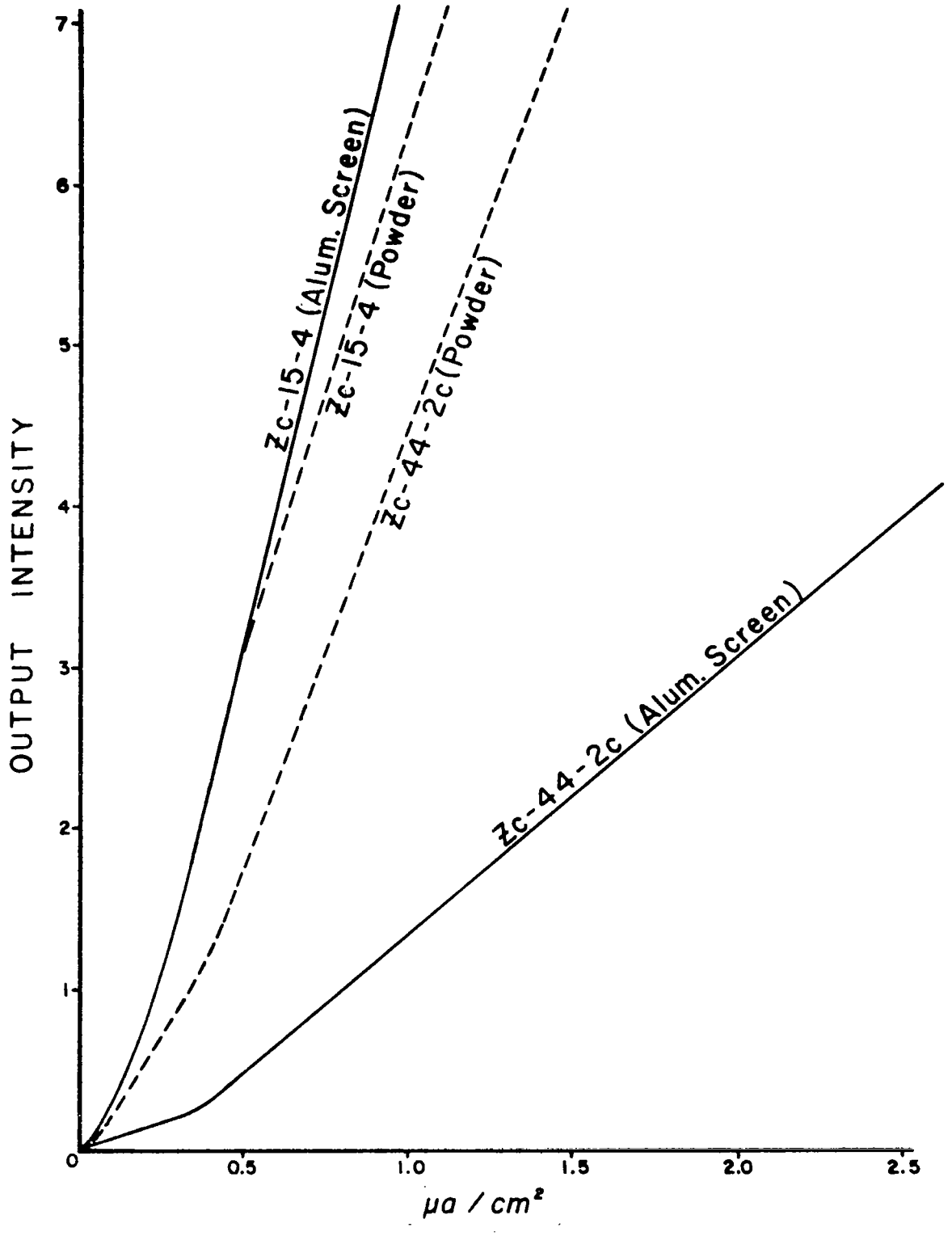

Figure 5B. Intensity Versus Current Density (Screen and Powder Data)

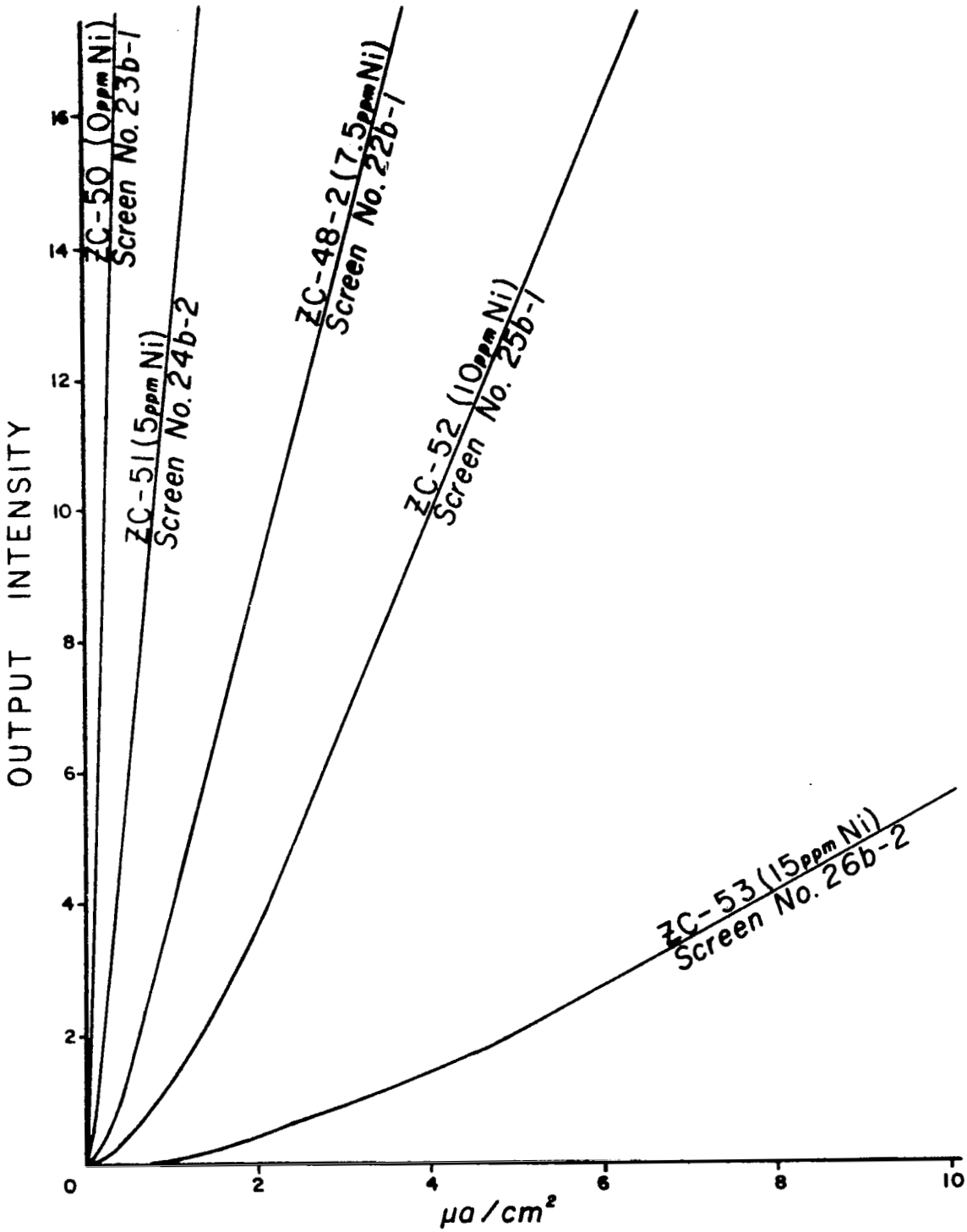

Figure 6A. Intensity Versus Current Density (Screen Data)

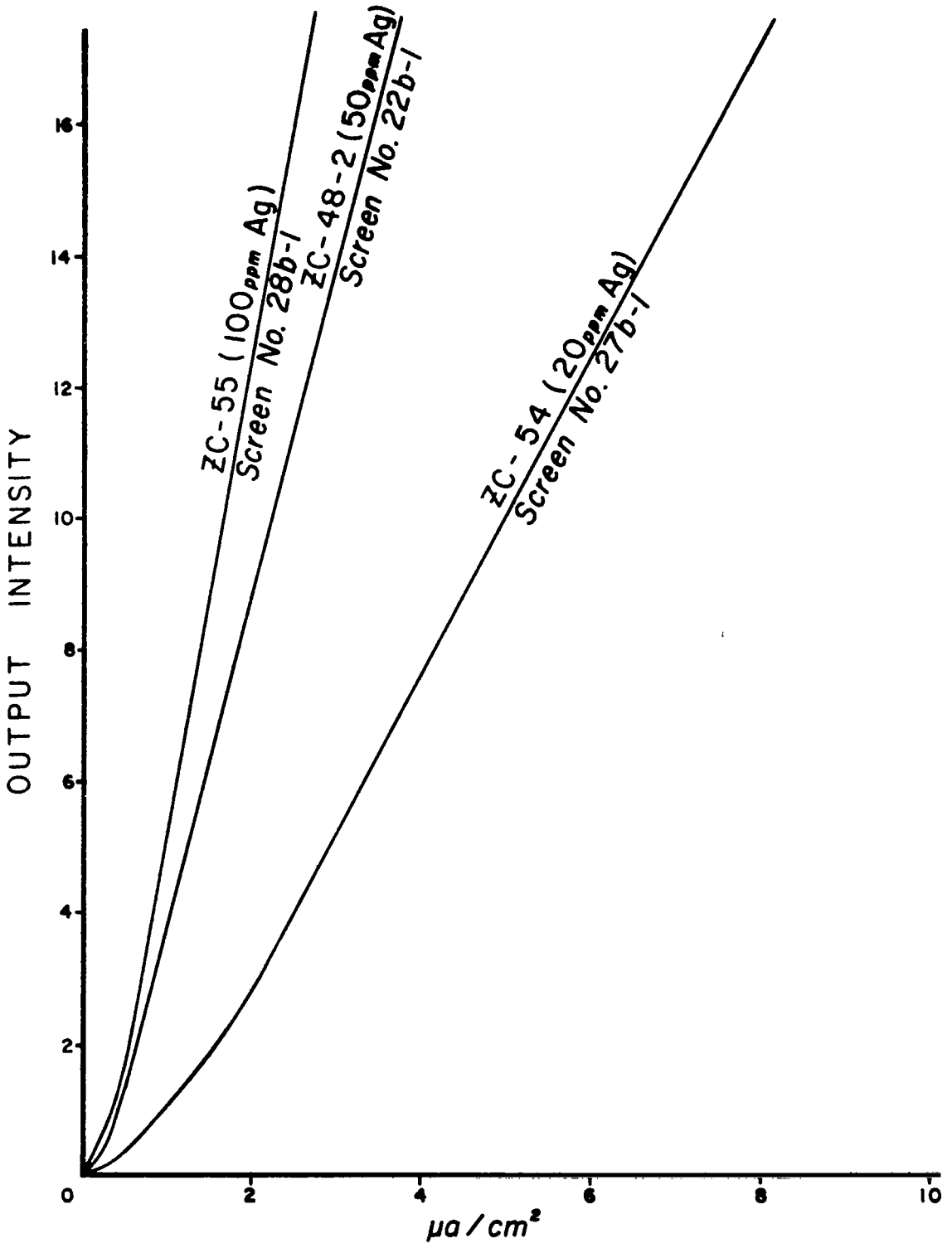

Figure 6B. Intensity Versus Current Density (Screen Data)

The evaluation of multiple firing techniques as a necessary procedure to obtain maximum superlinearity, also has been concluded with the evaluation of several identical samples in single firing experiments, in which both Ag and Ni were introduced at the same time. The most pronounced superlinearity was obtained employing a single firing procedure.

Superlinear sulfide red phosphors prepared by the multiple firing techniques produced a shift of the peak emission to longer wavelengths (deeper red). In addition, prefiring appears to induce a less stable SED for the red phosphors. The chromaticity coordinates shift to less saturated hues as the current density is decreased.

Mechanism of Superlinear Behavior

Work dealing with $(Zn_{.65}Cd_{.35})S$ as a host was performed in conjunction with company sponsored work in order to obtain some understanding of the luminescent mechanism operating in this material. Three materials were studied and had the general compositions $(Zn_{.65}Cd_{.35})S$:Ag:Ni. The samples differed in the amount of Ni present and firing times.

Sample	Nickel (ppm)
4a	0
4b	5
4c	9

The Ag content was 50 ppm. The material with no Ni present was used as a reference with respect to possible changes observed in the Ni doped materials.

Decay measurements were used in an attempt to observe possible changes in decay constant as a function of temperature and to determine if the decay were of the type e^{-at} or t^{-n}. Results indicated that for sample 4a, the decay curves were composed of two exponential portions (Figure 7). The decay was not t^{-n} as found in many of the sulfides. As the temperature was raised, the two curves were again observed and the data showed the curves to be parallel. Parallel curves indicate a temperature independent decay constant and suggest the decay is not coming from traps being emptied after light cessation. According to Leverenz, such behavior indicates emission within a single center. The decay constants were calculated to be 290 μsec and 225 μsec for the two portions of the curve. The presence of two linear portions suggests luminescence from two centers.

Decay constants for samples 4b and 4c containing Ni could not be measured with the present measuring system. The data indicated that the decay of these materials was equal to or less than the decay of the applied excitation (1-2 μsec).

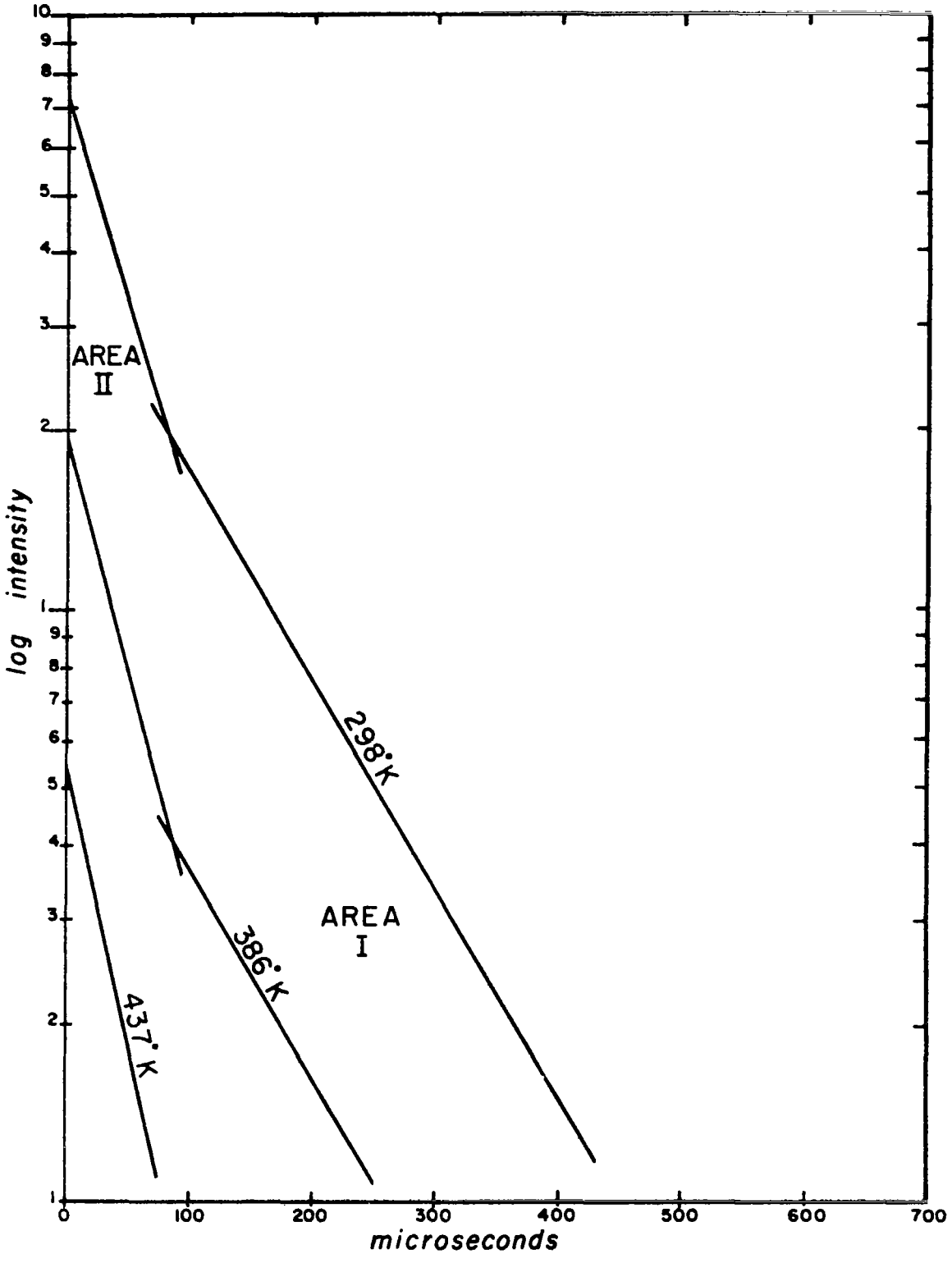

Figure 7. Decay Time Data for Sample 4a

Thermal quenching experiments were performed in an attempt to fix the terminal levels involved in the luminescence transitions. Figure 8 indicates the results obtained with sample 4a. Two activation energies were calculated, indicative of two quenching processes. The change in activation energy occurs at about 415°K and coincides with the temperature at which Process I decay ceases to be observable. Two centers are again suggested as producing the emission. Typical data for samples 4b and 4c are shown in Figures 9 and 10.

Changes in the luminescent spectra were studied as a function of temperature and indicated little if any change in the peak wavelength over the temperature range 300°K to 460°K. The data are shown in Figures 11, 12 and 13. The data are uncorrected but a shift to longer wavelengths is observed on Ni doped samples.

One concludes from these data that the luminescence from $(Zn_{.65}Cd_{.35})S$:Ag is probably caused by two separate centers represented as in Figure 14 with near identical energies.

The effect of Ni on this process is not entirely understood. The thermal data suggests values of the activation energies for luminescent quenching of Ni doped materials as 1.1 and 0.8 eV for 4b and 0.34 and 1.0 eV for 4c. The energies calculated indicate the Ni may introduce levels above the terminal level of the luminescence as shown in the figure. Consequently, in the absence of thermally excited electrons, these levels may serve as recombination centers to accept electrons from the conduction band more readily than the luminescent centers, and in this way may be responsible for the overall reduction in luminous intensity of Ni doped materials.

Sublinear Phosphors - Low Manganese Willemite Zn_2SiO_4

Earlier preprarations of low manganese Zn_2SiO_4 produced a useful sublinear phosphor suitable for screen preparation with a superlinear red phosphor. However, later preparations were not as reproducible, yielding phosphors with both the characteristic blue of unactivated Zn_2SiO_4, and green emission characteristic of manganese. The homogeneous distribution of manganese in the raw material is the principal difficulty, which can be overcome by use of proper techniques for the incorporation of manganese. The data for the best Zn_2SiO_4:Mn phosphors prepared is given in Appendix A for powders, and Appendix B for screens. Plots of intensity versus current density are illustrated in Figure 15 for several powder samples.

Modified $Zn_3(PO_4)_2$:Mn Red Phosphors

Zinc phosphate activated with manganese yields a red phosphor. At low manganese concentrations the red emission can be maintained through the addition of a small amount of cadmium to the sample. Very good sublinear emission was obtained from these phosphors. Sample screens, reported in Appendix B, were prepared and evaluated. This phosphor has been combined with a superlinear green phosphor to form the screens for the last Quarterly tube. (Q-2)

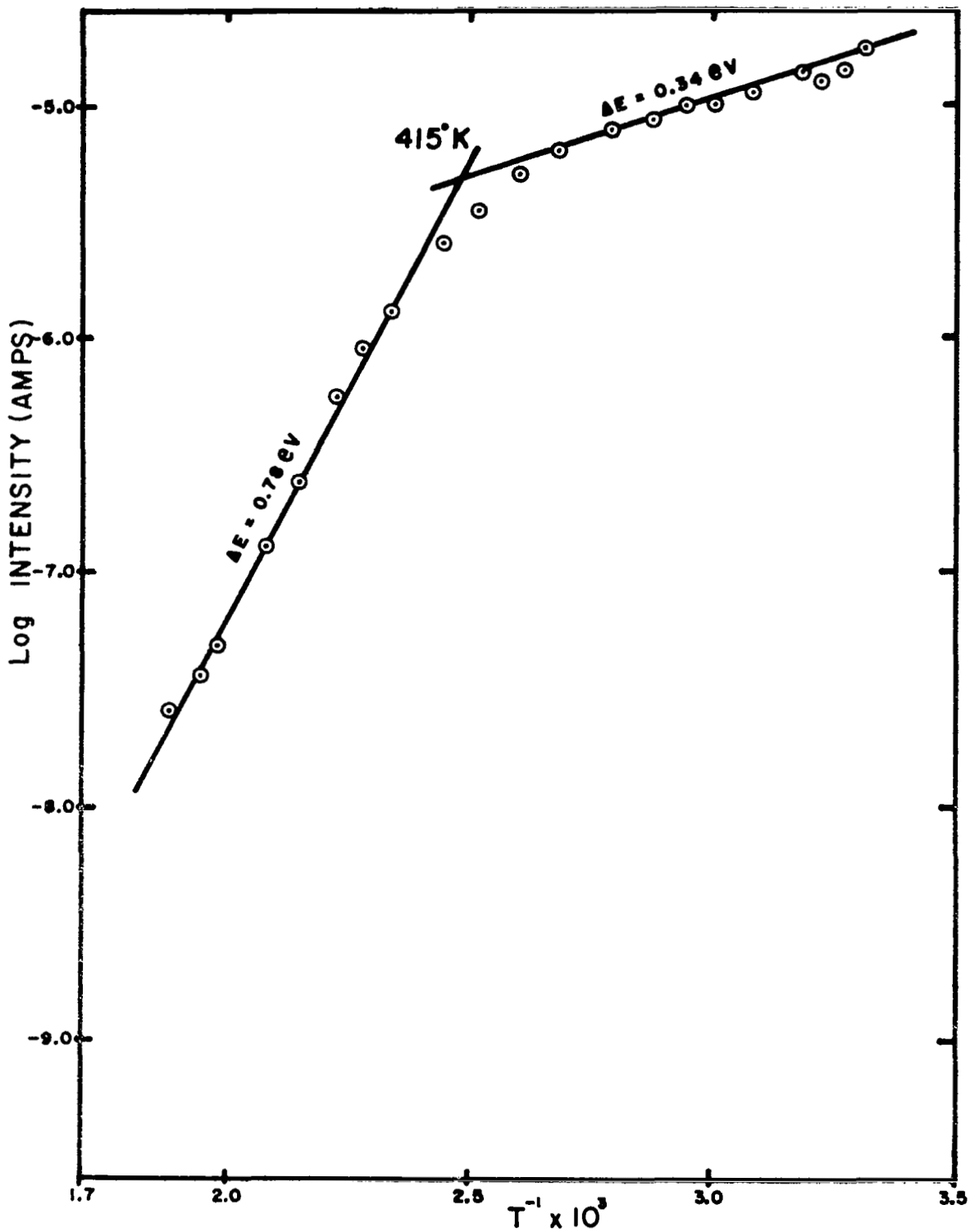

Figure 8. Thermal Quenching for Sample 4a

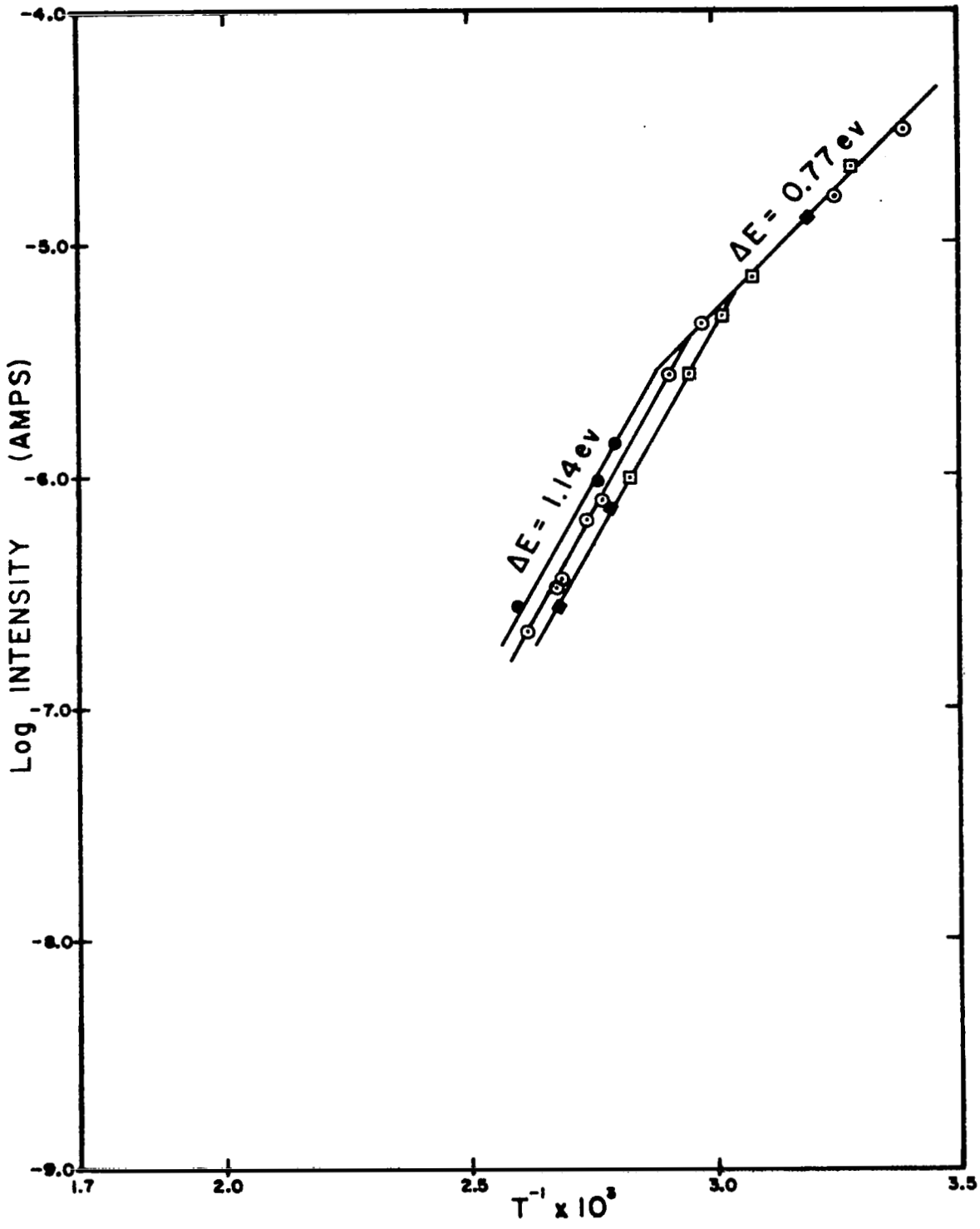

Figure 9. Thermal Quenching for Sample 4b

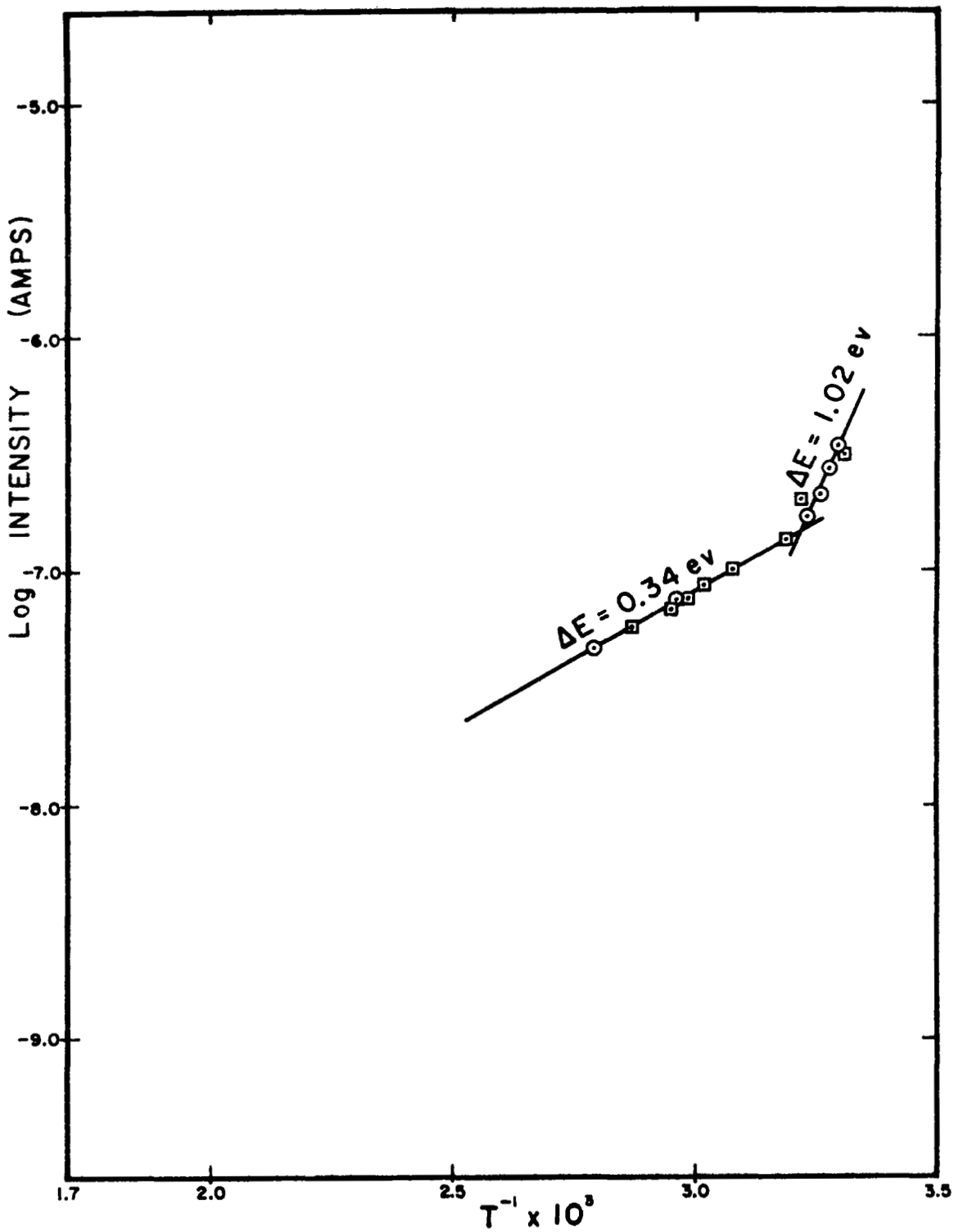

Figure 10. Thermal Quenching for Sample 4c

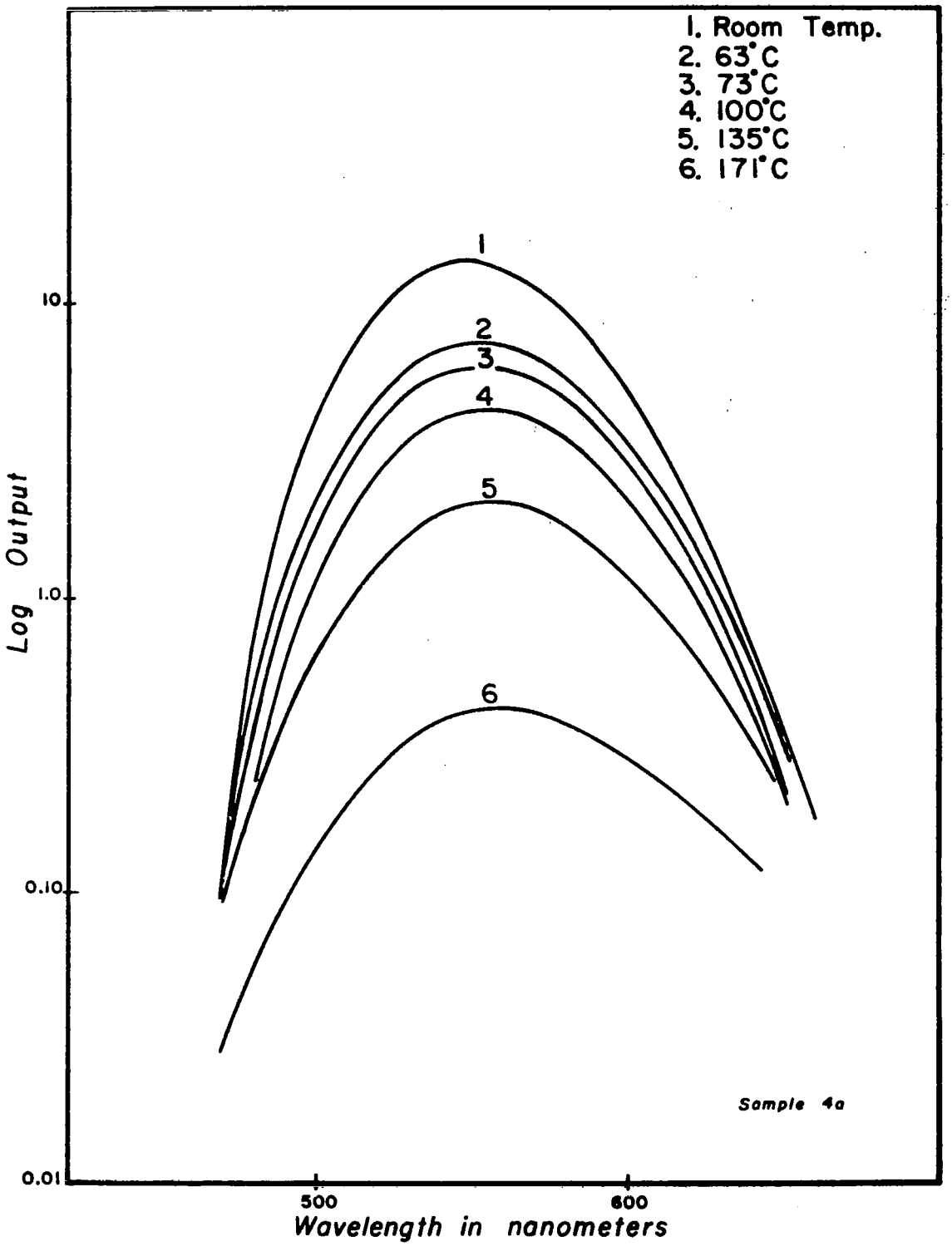

Figure 11. Thermal Spectra for Sample 4a

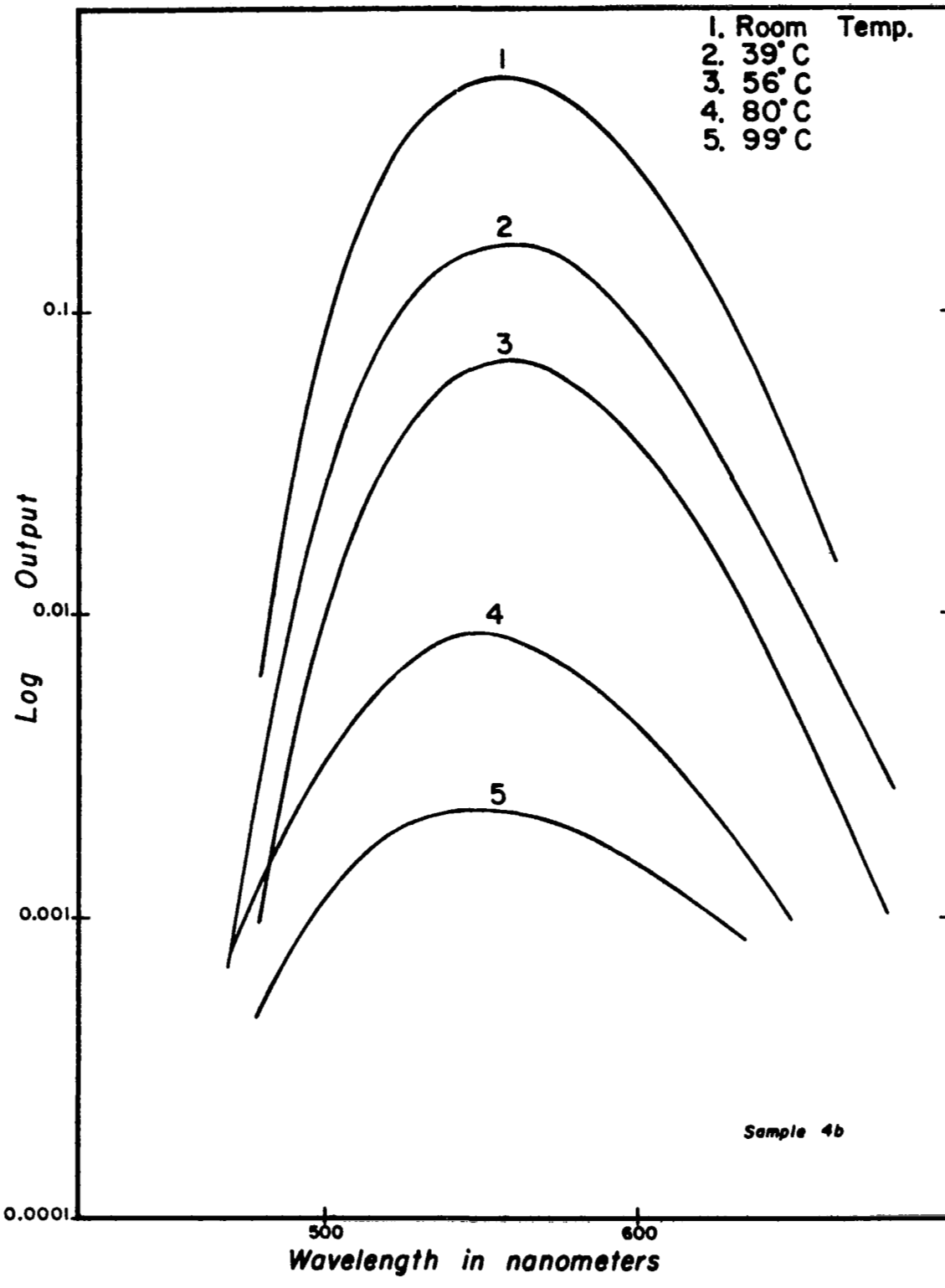

Figure 12. Thermal Spectra for Sample 4b

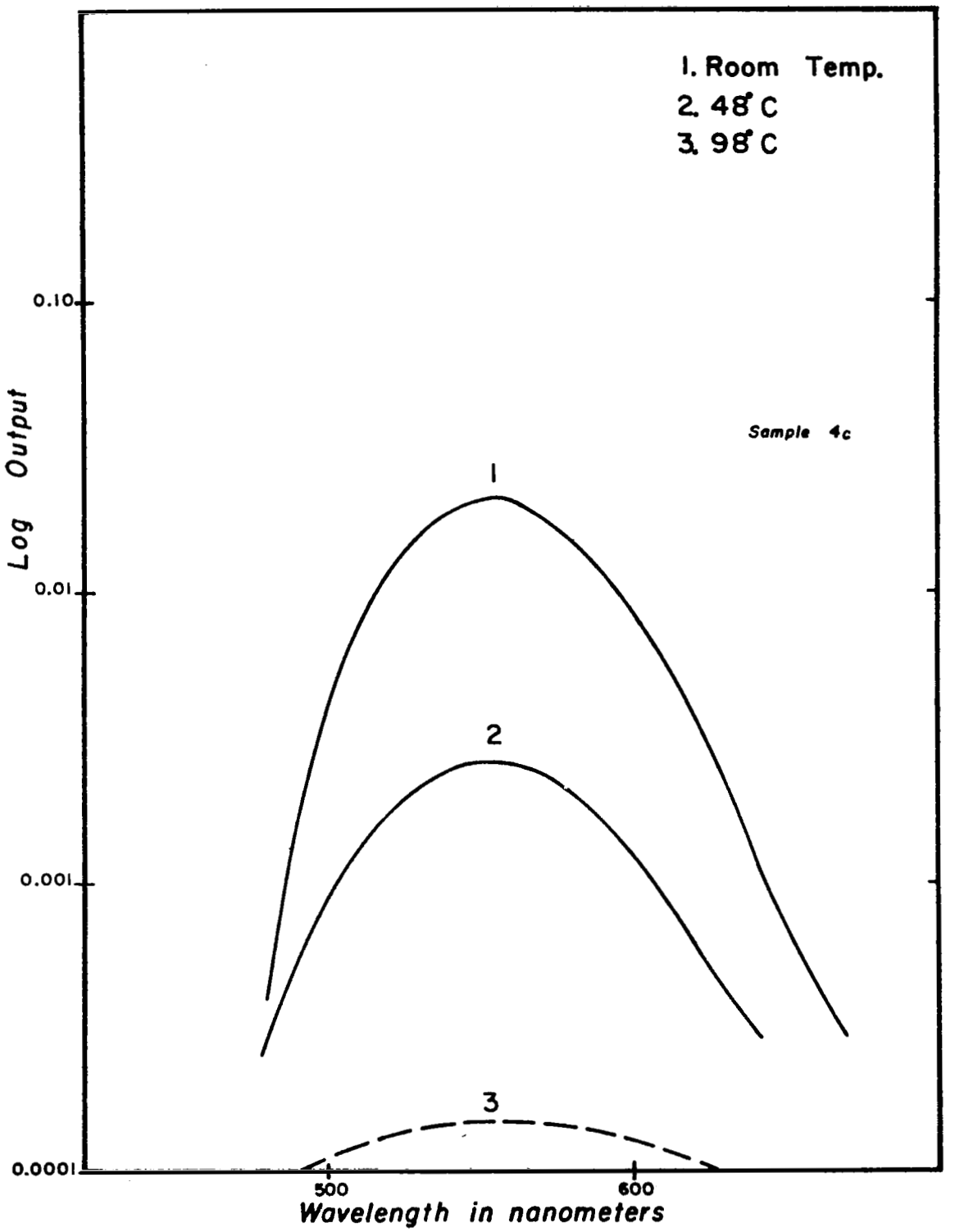

Figure 13. Thermal Spectra for Sample 4c

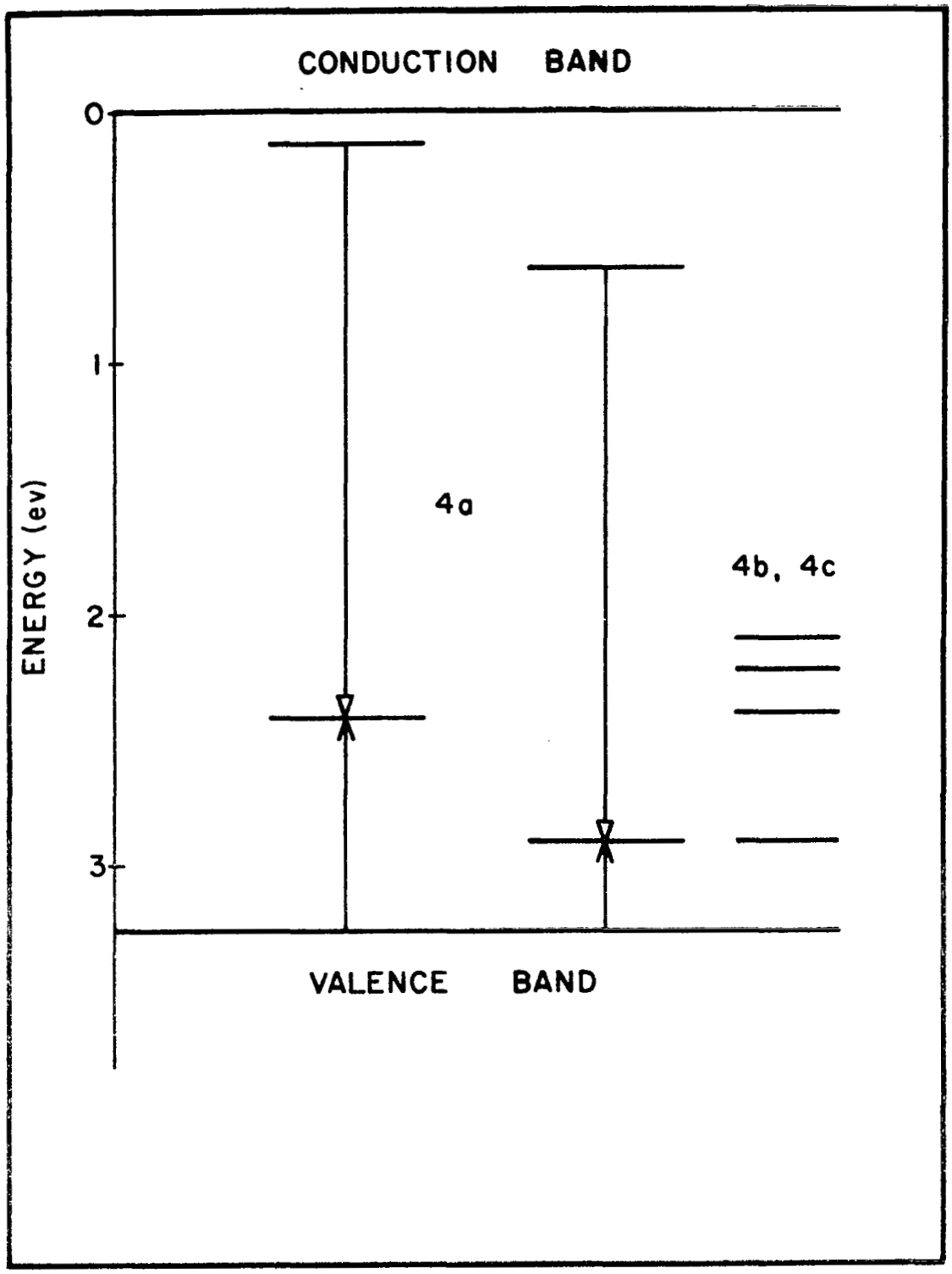

Figure 14. Possible Energy Diagram for Two Color Phosphor

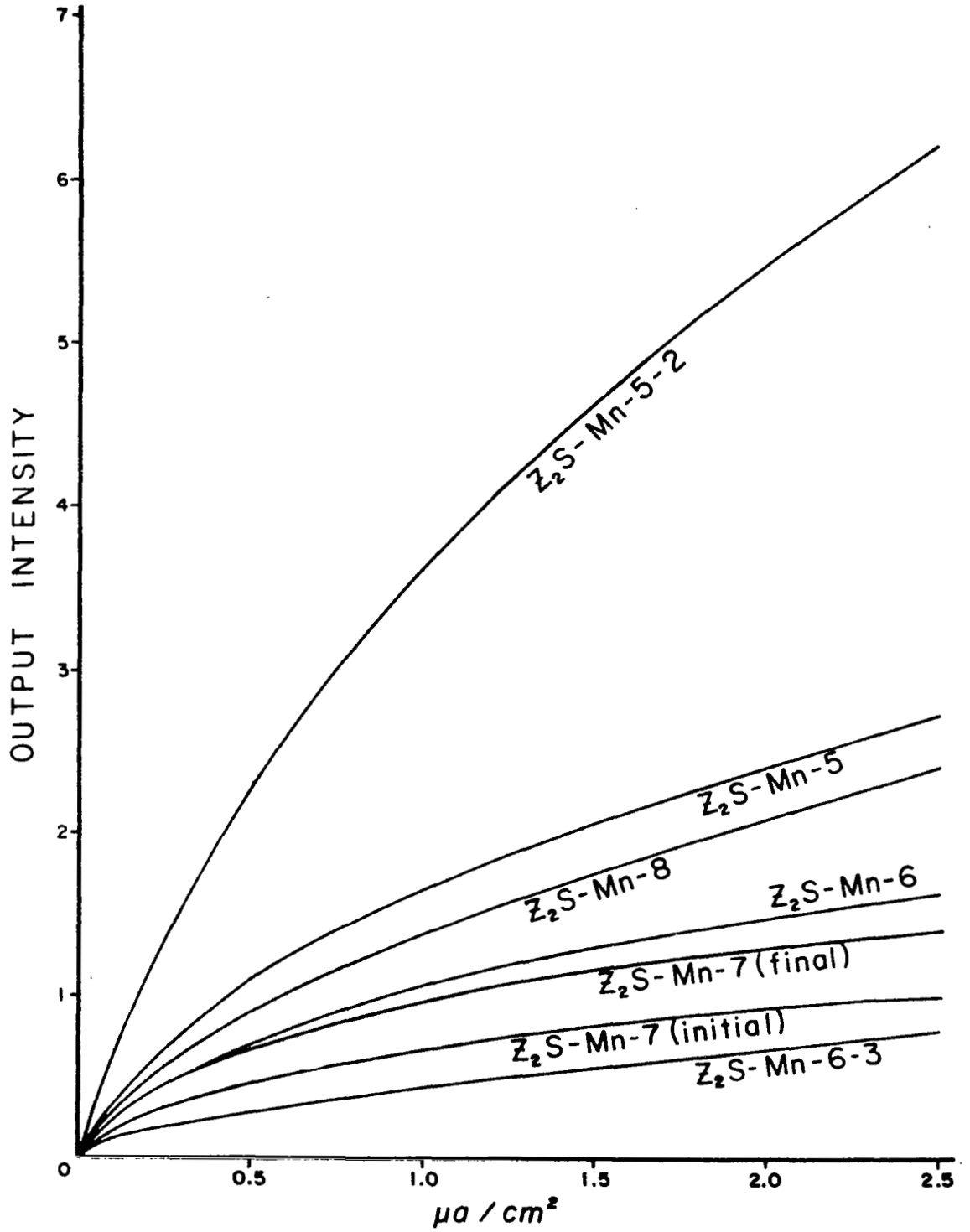

Figure 15. Intensity Versus Current Density (Powder Data)

The phosphor output intensity-current density plots are shown in Figure 16 for powder sample and the data tabulated in Appendices A and B for the $Zn_3(PO_4)_2$:Mn red phosphors.

Re-evaluation of Phosphors for Sublinear Behavior

A number of red and green phosphors prepared in the past year were re-examined to determine whether the indicated sublinear characteristic of powders would remain in screens. Powder sample evaluation had indicated that pronounced sublinear behavior occurred at current densities greater than 1 $\mu a/cm^2$. The screen evaluation revealed this pronounced sublinearity was not observed when the screen output intensity versus current density was measured. Figure 17 illustrates several red phosphor screen outputs versus current density. Samples CZ66 and CZ67 do display a sublinear characteristic. These phosphors were employed in the preparation of a number of screens prior to tube fabrication.

Other Phosphor Systems - Thulium Activated ZnS With Ni

Superlinearity is most pronounced in (Zn, Cd)S:Ag:Ni phosphors within the range of Zn/Cd weight ratio of approximately 2.3 to 0.43. The emission color ranges from blue-green to orange. Investigations of the behavior of lanthanide activated sulfides was initiated with one of the more efficient host crystal-activator pairs; namely, ZnS:Tm. The phosphor synthesis was accomplished by firing in a H_2S atmosphere. After the optimum temperature and thulium concentration were established, nickel was added in varying amounts. Nickel decreases the intensity, but does not produce a superlinear brightness versus current density characteristic.

(Zn, Cd)S:Tm:Ni Compositions

Green and red emitting compositions of zinc and cadmium sulfide containing thulium were prefired in H_2S with and without nickel, followed by a normal air firing with silver and NaCl flux. Both the firing and prefiring steps were carried out at several temperatures and times. The powder sample data are reported in Appendix A and screen data in Appendix B. Note that all exhibit superlinearity as shown in Figures 18A and 18B. Figure 18A illustrates the superlinearity of the green emitting phosphor compared to one of the best superlinear phosphors previously prepared. The data clearly shows the H_2S firing produces superlinearity as well as, but not better than, the conventional method.

Lanthanide Activated Phosphors

A series of terbium activated borates were prepared and evaluated on both powder and screen form. The compositions studied were Li La B_2O_5 Li/B_2O_5 and Li In B_2O_5. The screen data, tabulated in Appendix B, revealed no superlinear or sublinear properties. The brightness versus current density characteristic was quite linear and the brightness was too high for use as a sublinear component.

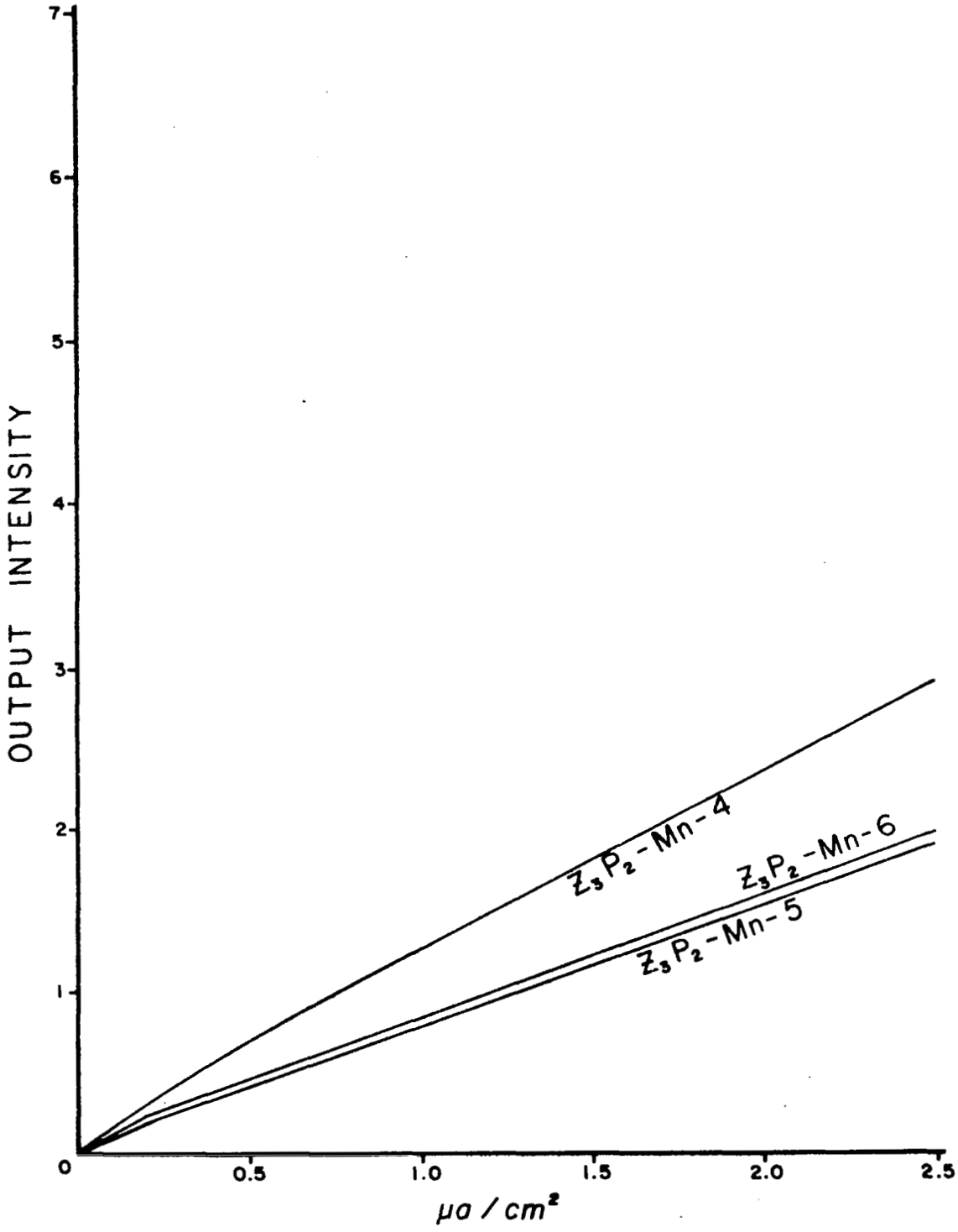

Figure 16. Intensity Versus Current Density (Powder Data)

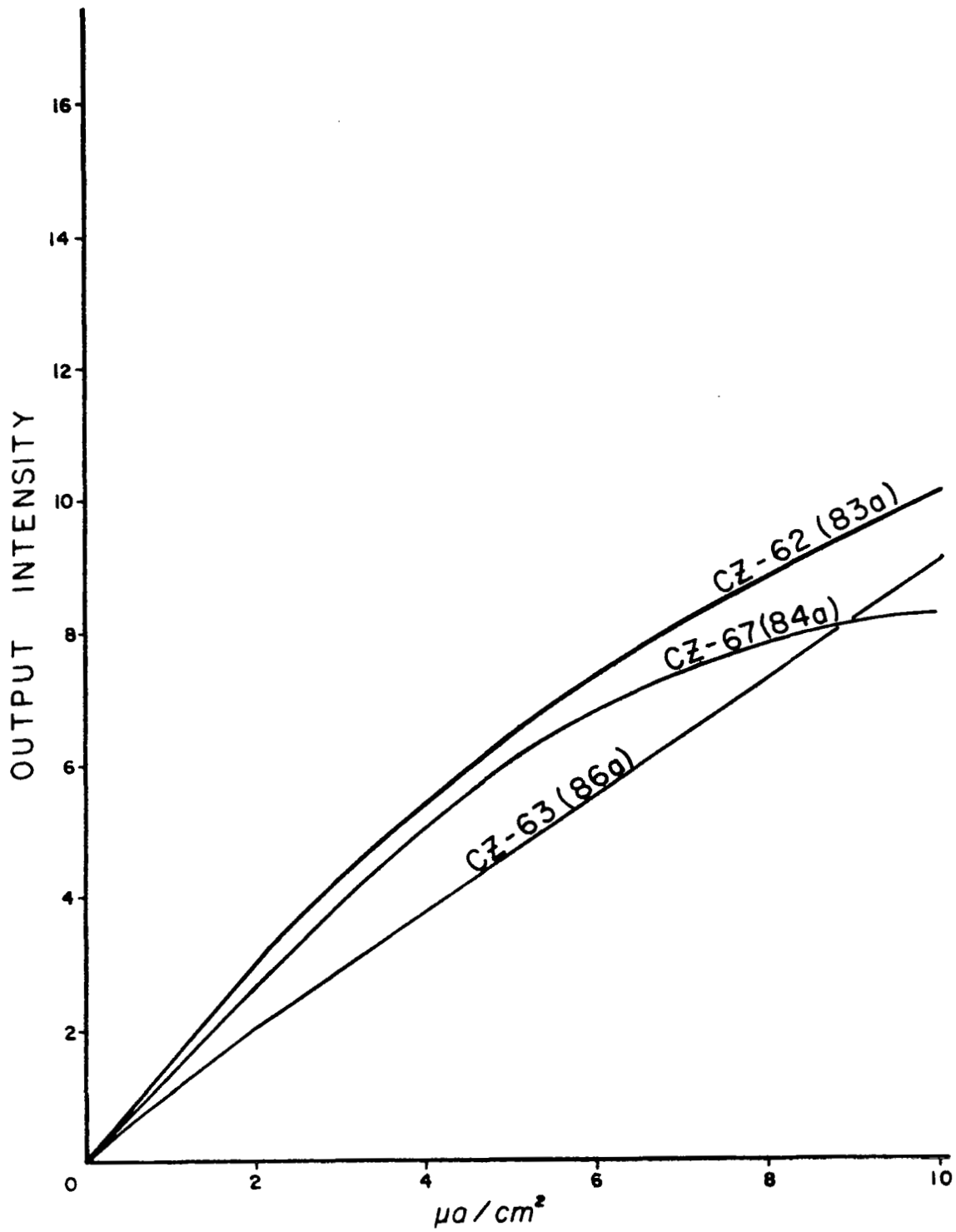

Figure 17. Intensity Versus Current Density (Screen Data)

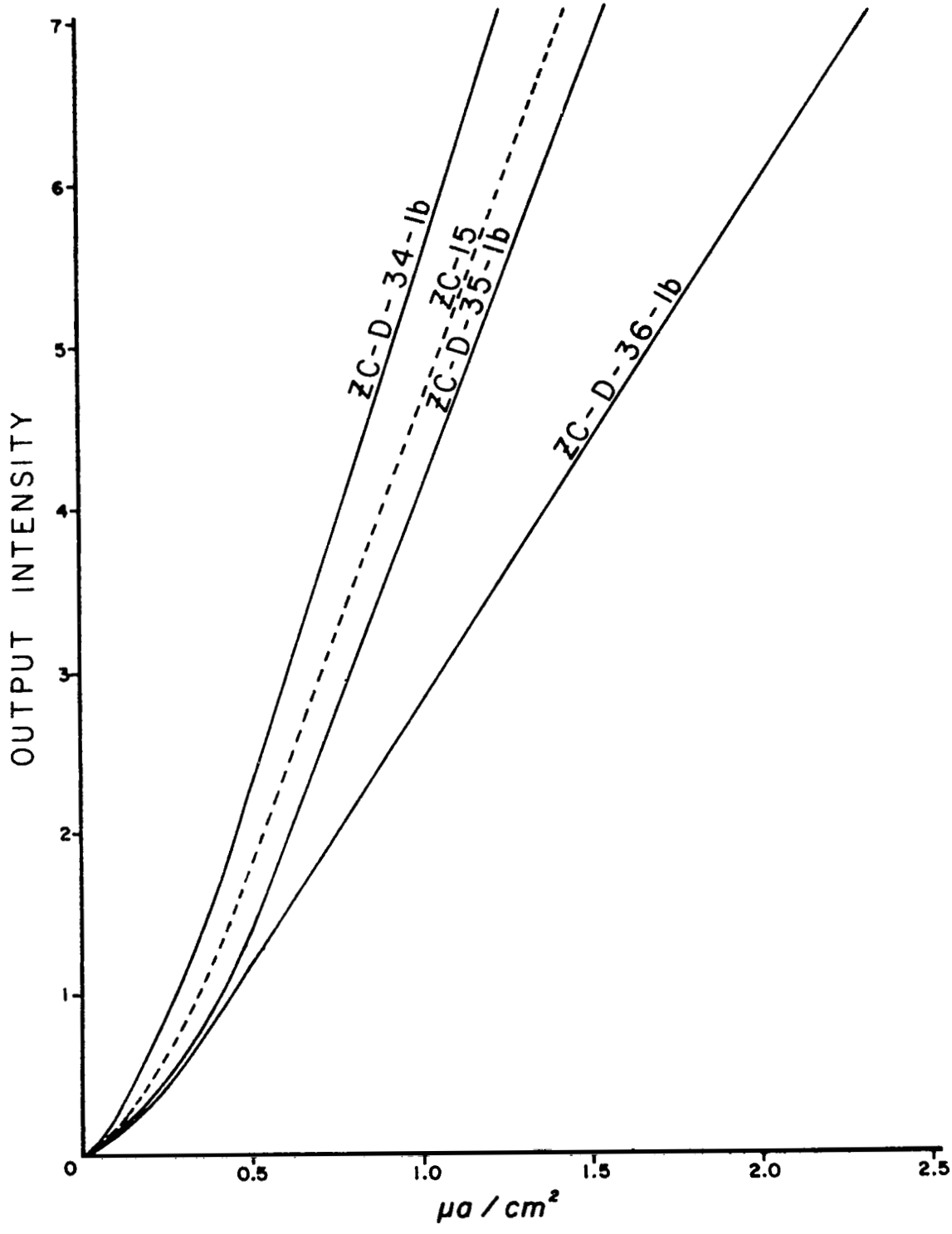

Figure 18A. Intensity Versus Current Density (Powder Data)

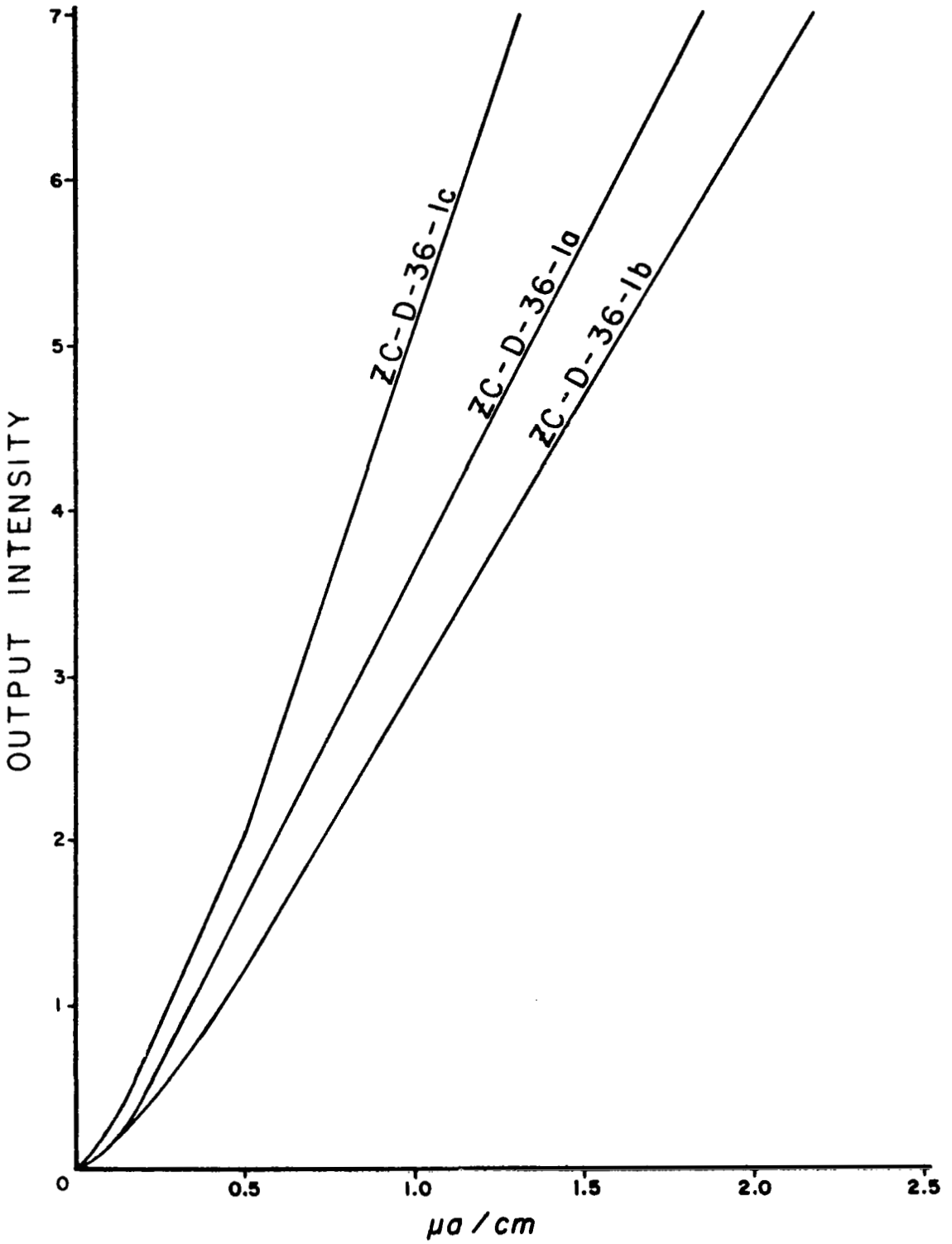

Figure 18B. Intensity Versus Current Density (Powder Data)

Silicate host crystal phosphors with blue emission containing terbium, with the composition $Ba/Zn_2Si_2O_7$, were also evaluated for their brightness versus current density behavior. These phosphors exhibited a linear behavior and did not show a change of intensity of the blue Tb bands.

UV Emitting Phosphors

Two ultraviolet emitting phosphors, developed by ITT, referred to by GB and JJ code designations, were evaluated for nonlinear behavior. Neither phosphor exhibited a superlinear brightness versus current density, but both materials had slight sublinear behavior.

Screen Evaluation - Comparison of Screen and Powder Characteristic

It has been emphasized earlier that variations between powder data and the anticipated screen chromaticity coordinates and output intensity made it necessary to evaluate single phosphors in addition to phosphor mixtures in screens before choosing a phosphor composition for CRT's.

The differences between powder and screen data are clearly illustrated by comparing intensity ratios and chromaticities for individual phosphors in Appendices A and B, Figure 5B also illustrates the variance encountered due to preparation conditions for ZC15-4 and ZC44-2. Note the large differences between screen and powder output intensity versus current density for ZC44-2C, while the agreement for powder and screen intensity versus current density data for ZC15-4 is quite good. Phosphor particle size differences may account for this large difference, although, firing in H_2S may also prove to exert a great influence on this behavior.

An examination of the data in Appendices A and B for the same sample reveals the powder data yields in general a lower intensity ratio than the corresponding screen data. However, the screen data roughly parallels the powder intensity ratio. (Compare ZC48-2 to 57 green phosphors and CZ87-92 red phosphors) in Appendix A with the data in Appendix B.

Screen Evaluation - Effect of Current Density

The phosphor screens evaluation studies revealed a number of superlinear green sulfides exhibited a pronounced color shift with current density. This shift produces slightly less saturated hues at low current density; however, as the current density increases the color shift of the superlinear green is toward more saturated hues (higher x and y chromaticities) and hence the colors attainable at higher current densities become more saturated. The data illustrating the effect is given in Appendix B.

Screen Evaluation - Vacuum Bake Studies

Vacuum baking experiments were conducted on single phosphor screens. Disagreement between screen and tube chromaticity versus current density results and between phosphor powder and screen intensity data indicated a change in these phosphor characteristics was taking place.

The exhaustive tests run on numerous single phosphor screens revealed the effect on phosphor chromaticity is practically negligible. Intensity measurements are difficult to interpret due to variation in screen coverage. It was established that reducing bake out time did improve tube characteristics.

Screens With Two Phosphors

The chromaticity data given in Appendix B for screens prepared with phosphor mixtures is given primarily for completeness and is therefore not discussed. The quarterly tubes prepared in this study contained phosphor screen compositions based on the evaluation made on these screens.

QUARTERLY TUBES

Data for the four 5-inch CRTs delivered during this contract are reported in Appendix C. The color gamut for these tubes, designated K-1, M-I-A, M-I-B, O-1 and Q-2 is represented on the Kelley Diagrams shown in Figures 19A and 19B. The numbers given on these figures are the current densities required to produce the chromaticity coordinates.

BIBLIOGRAPHY

1. Sisneros T. E., Faeth P. A., and Davis, J. A., Research and Development of a single gun color CRT. Phase I Final Report. NASA CR1228. Dec. 1968.

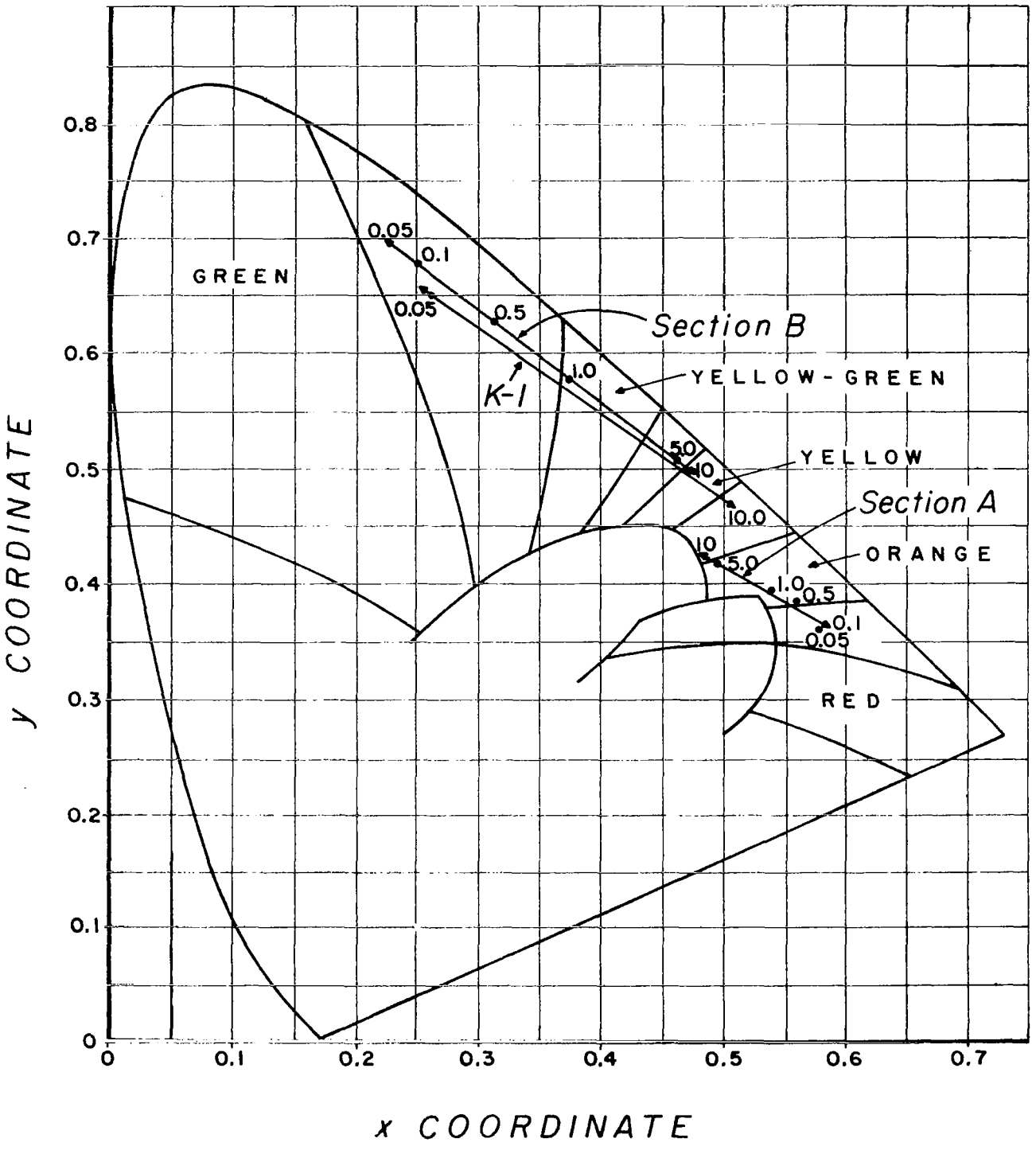

Figure 19A. Color Gamut of Quarterly Tubes K-1, M-1A and M-1B

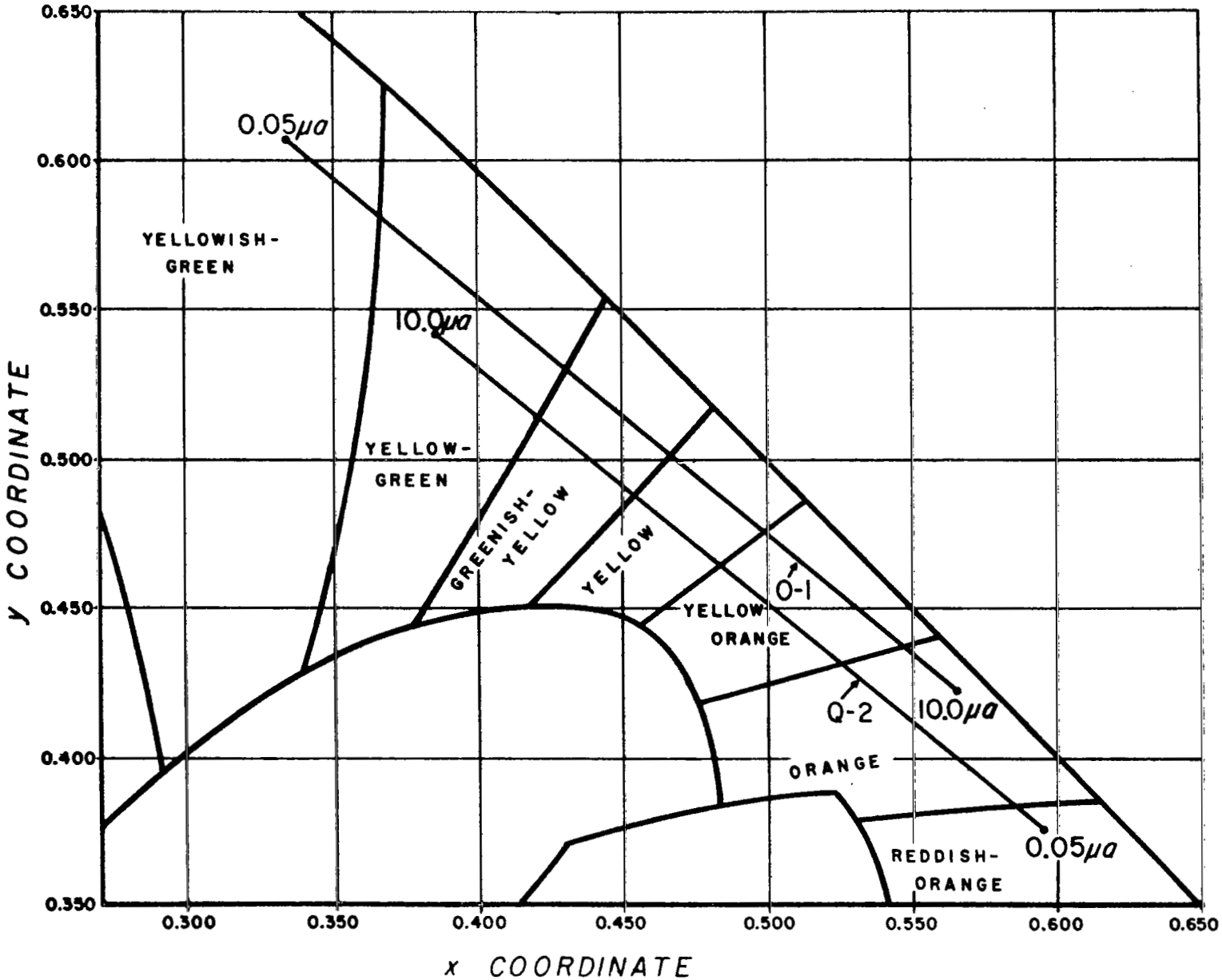

Figure 19B. Color Gamut of Quarterly Tubes O-1 and Q-2

APPENDICES

The information in Appendix A is for the most part self explanatory. However, several headings have been simplified to avoid repetition. These are as follows:

a. Weight ratio Zn/Cd is the composition of the mixture of ZnS and CdS by weight.

b. Firing conditions are listed with the firing time given in hours followed by the temperature in Centigrade degrees.

   For samples with two firing times and temperatures indicated, the first firing was conducted with nickel present. The second firing was carried out with the silver or other activators present.

c. Flux compound employed in each firing contained 1 percent by weight of the indicated compound.

d. The Peak Wavelength listed is given in nanometers.

e. The intensity data is the output in microamperes of a 1-P21 photomultiplier - Wratten 106 filter combination adjusted to read 10.0 μa output intensity for a standard P-1 phosphor. The output intensity is measured at 1.0 $\mu a/cm^2$ beam current and 10 kv beam voltage. Note in Phase I report, 0.5 μa/cm was the normal beam current density.

f. The intensity ratio is a measurement of the degree of super-linear or sublinear character of the phosphor in the 0.05 to 1.0 $\mu a/cm^2$ range of beam current density. The output intensity at a beam current of 1.0 $\mu a/cm^2$ is divided by the output intensity at 0.05 $\mu a/cm^2$ beam current. A ratio of 20 would signify a linear intensity versus beam current density, while a ratio of less than 20 indicates a sublinear character and a ratio of more than 20 indicates a super-linear output versus current density.

APPENDIX A

POWDER PHOSPHOR DATA

I Superlinear Green Compositions

Number	Wgt Ratio Zn/Cd	Ag ppm	Ni ppm	Firing Conditions Time-Temp	Flux	Peak wavelength (nm)	Intensity at 1 $\mu a/cm^2$	Intensity Ratio	Comments
ZC-D8-I	1.0	50	2	2h-750 2h-750	NaF NaCl	550	9.7	21	Double firing.
ZC-D8-II	1.0	50	2	2h-750 2h-850	NaF NaCl	554	9.8	23	Double firing.
ZC-D9-I	1.0	50	2	2h-850 2h-750	NaF NaCl	557	9.7	27	Double firing.
ZC-D9-II	1.0	50	2	2h-850 2h-850	NaF NaCl	553	8.0	23	Double firing.
ZC-D10-I	1.0	50	4	2h-750 2h-750	NaF NaCl	555	18.2	23	Double firing.
ZC-D10-II	1.0	50	4	2h-750 2h-850	NaF NaCl	555	12.5	23	Double firing.
ZC-D11-I	1.0	50	8	2h-750 2h-750	NaF NaCl	555	9.7	31	Double firing.
ZC-D11-II	1.0	50	8	2h-750 2h-850	NaF NaCl	550	9.0	38	Double firing.

APPENDIX A (Continued)

Number	Wgt Ratio Zn/Cd	Ag ppm	Ni ppm	Firing Conditions Time-Temp	Flux	Peak wavelength (nm)	Intensity at 1 $\mu a/cm^2$	Intensity Ratio	Comments
ZC-D34-1a	1.5	50	7.5	2h-1000 3h-750	H_2S NaCl	529	4.2	45	(
ZC-D34-1b	1.5	50	7.5	2h-1000 3h-850	H_2S NaCl	529	5.5	52	(
ZC-D34-1c	1.5	50	7.5	2h-1100 3h-950	H_2S NaCl	543	7.9	58	(Thulium in H_2S firing step, (Ag + Ni added in second firing (step with NaCl flux. No effect
ZC-D35-1a	1.5	50	7.5	2h-1100 3h-750	H_2S NaCl	542	3.2	56	(from Tm. (
ZC-D35-1b	1.5	50	7.5	2h-1100 3h-850	H_2S NaCl	531	4.1	69	((
ZC-D35-1c	1.5	50	7.5	2h-1100 3h-950	H_2S NaCl	531	6.5	54	((
ZC-E-4	1.22	50	7.5	2h-850	NaCl	542	40.0	14	(
ZC-E-5	1.22	50	7.5	2h-850	NaCl	543	40.0	14	(Three duplicates to determine (uniformity.
ZC-E-6	1.22	50	7.5	2h-850	NaCl	540	38.5	14	((
ZC-D36-3a	1.0	50	7.5	2h-1100 3h-750	H_2S NaCl	536	2.9	81	(
ZC-D36-3b	1.0	50	7.5	2h-1100 3h-850	H_2S NaCl	527	2.6	47	(Ni and Tm introduced in H_2S (firing.
ZC-D36-3c	1.0	50	7.5	2h-1100 3h-950	H_2S NaCl	534	4.2	54	((

APPENDIX A (Continued)

Number	Wgt Ratio Zn/Cd	Ag ppm	Ni ppm	Firing Conditions Time-Temp	Flux	Peak wavelength (nm)	Intensity at 1 $\mu a/cm^2$	Intensity Ratio	Comments
ZC-44-2a	1.0	50	7.5	2h-1100 3h-750	H_2S NaCl	537	2.6	54	(
ZC-44-2b	1.0	50	7.5	2h-1100 3h-850	H_2S NaCl	523	2.6	42	(Repeat of ZC-D36 without Thulium
ZC-44-2c	1.0	50	7.5	2h-1100 3h-950	H_2S NaCl	534	3.4	47	(
ZC-45-B	1.35	50	7.5	2h-1100 3h-950	H_2S NaCl	505	0.88	38	
ZC-47	1.50	50	7.5	3h-1000 3h-850	H_2S $CaCl_2$	524	6.0	35	
ZC-15-4	1.2	50	7.5	2h-850	NaCl	525	6.4	49	
ZC-48-2	1.2	50	7.5	2h-850	$CaCl_2$	540	4.7	70	(
ZC-48	1.2	50	7.5	2h-850	$CaCl_2$	540	5.5	60	(Same as ZC15-4 but with different flux.
ZC-49	1.2	50	7.5	2h-850	KBr $BaBr_2$	540	9.8	44	(
ZC-50	1.2	50	0	2h-850	$CaCl_2$	540	54.0	20	
ZC-51	1.2	50	5	2h-850	$CaCl_2$	540	15.0	42	
ZC-52	1.2	50	10	2h-850	$CaCl_2$	538	1.7	73	
ZC-53	1.2	50	15	2h-850	$CaCl_2$	535	0.29	50	

APPENDIX A (Continued)

Number	Wgt Ratio Zn/Cd	Ag ppm	Ni ppm	Firing Conditions Time-Temp	Flux	Peak wavelength (nm)	Intensity at $1\mu a/cm^2$	Intensity Ratio	Comments
ZC-54	1.2	20	7.5	2h-850	$CaCl_2$	540	1.1	73	
ZC-55	1.2	100	7.5	2h-850	$CaCl_2$	540	8.7	60	
ZC-56	1.2	200	7.5	2h-850	$CaCl_2$	540	10.0	49	
ZC-57	1.2	200	15	2h-850	$CaCl_2$	530	0.78	65	
ZC-58	1.0	50	7.5	2h-850	NaCl	-	-	-	+ 50 ppm Cu

APPENDIX A (Continued)

II Superlinear Red Compositions

Number	Wgt Ratio Zn/Cd	Ag ppm	Ni ppm	Firing Conditions Time-Temp	Flux	Peak wavelength (nm)	Intensity at 1 $\mu a/cm^2$	Intensity Ratio	Comments
CZ-G-4	0.43	50	7.5	3h-950	NaCl	624			(
				2h-750	NaCl				(
									(
CZ-G-5	0.43	50	7.5	3h-950	NaCl	624	13.5	15	(
				2h-750	NaCl				(First firing with Ag; 2d
									(firing with Ni.
CZ-G-6	0.43	50	7.5	3h-950	NaCl	624			(
				2h-750	NaCl				(
CZ-39-2	0.43	50	7.5	2h-850	NaCl	634	1.95	51	(Prefiring shifts emission to
				2h-850	NaCl				(longer λ.
									(The Ni is added in first firing
CZ-40-2	0.25	50	7.5	2h-850	NaCl	656	0.91	25	(and the Ag in the second firing.
				2h-850	NaCl				(
									(
CZ-74	0.43	50	7.5	3h-950	NaCl	672	0.76	22	(
				2h-850	NaCl				(
CZ-61-12	0.43	50	7.5	3h-950	NaCl	635	1.0	44	Repeat of 61-1
				2h-750	NaCl				
CZ-76-a	0.43	50	7.5	2h-800	H_2S	635	1.6	28	
				3h-650	NaCl				
CZ-76-b	0.43	50	7.5	2h-800	H_2S	614	1.9	34	
				3h-750	NaCl				
CZ-76-c	0.43	50	7.5	2h-800	H_2S	613	2.0	37	
				3h-850	NaCl				

APPENDIX A (Continued)

Number	Wgt Ratio Zn/Cd	Ag ppm	Ni ppm	Firing Conditions Time-Temp	Flux	Peak Wavelength (nm)	Intensity at $1\mu a/cm^2$	Intensity Ratio	Comments
CZ-77-a	0.43	50	7.5	2h-900 3h-650	H_2S NaCl	642	1.2	26	
CZ-77-b	0.43	50	7.5	2h-900 3h-750	H_2S NaCl	638	1.45	29	
CZ-77-c	0.43	50	7.5	2h-900 3h-850	H_2S NaCl	626	0.92	28	
CZ-78-a	0.43	50	7.5	3h-750 3h-650	H_2S NaCl	653	1.1	35	
CZ-78-b	0.43	50	7.5	3h-750 3h-750	H_2S NaCl	653	1.1	46	
CZ-78-c	0.43	50	7.5	3h-750 3h-850	H_2S NaCl	653	1.2	51	
CZ-79-a	0.43	50	7.5	3h-850 3h-650	H_2S NaCl	653	1.1	38	
CZ-79-b	0.43	50	7.5	3h-850 3h-750	H_2S NaCl	653	1.15	55	
CZ-79-c	0.43	50	7.5	3h-850 3h-850	H_2S NaCl	653	1.1	53	
CZ-81-A	0.43	50	7.5	3h-1000 3h-750	H_2S $CaCl_2$	676	1.45	17	((Sample heterogeneous (81-A - Top
CZ-81-B	0.43	50	7.5	3h-1000 3h-750	H_2S $CaCl_2$	650	0.42	30	(81-B - Bottom (
CZ-82	0.43	50	7.5	3h-950 2h-750	H_2S NaCl	640	0.7	41	

APPENDIX A (Continued)

Number	Wgt Ratio Zn/Cd	Ag ppm	Ni ppm	Firing Conditions Time-Temp	Flux	Peak Wavelength (nm)	Intensity at 1 $\mu a/cm^2$	Intensity Ratio	Comments
CZ-83	0.43	50	7.5	3h-950 2h-750	H_2S $ZnCl_2$	680	0.42	14	
CZ-84	0.43	50	7.5	3h-950 2h-750	H_2S $CdCl_2$	680	0.71	18	
CZ-85	0.43	50	7.5	3h-950 2h-750	H_2S $KBr+BaBr_2$	620	0.46	26	
CZ-86	0.43	50	7.5	3h-950 2h-750	H_2S $KBr+CaBr_2$	630	0.9	38	
CZ-87	0.43	50	7.5	2h-800	NaCl	620	1.2	92	
CZ-88	0.43	50	7.5	2h-800	$CaCl_2$	630	1.2	78	
CZ-89	0.43	50	7.5	2h-800	$KBr+BaBr_2$	625	0.9	80	
CZ-90	0.43	50	7.5	3h-850	$CaCl_2$	630	1.55	60	
CA-91	0.43	50	7.5	3h-850 2h-750	$CaCl_2$ $CaCl_2$	625	1.0	52	
CZ-92	0.43	50	7.5	3h-850 2h-750	$KBr+BaBr_2$ $KBr+BaBr_2$	630	1.7	63	Ni added in first firing and Ag in second.
CA-93	0.43	50	7.5	3h-600 2h-800	$KBr+BaBr_2$ $KBr+BaBr_2$	640	2.85	60	
CA-93-1	0.43	50	7.5	3h-600 2h-800	$KBr+BaBr_2$ $KBr+BaBr_2$	635	3.20	51	

APPENDIX A (Continued)

III Oxide Based Phosphors

Number	Composition	Activator and Concentration		Firing Time-Temp	Peak Wavelength (nm)	Intensity $1\,\mu a/cm^2$	Intensity Ratio	Comments
$LiLB_2$-Tb-5	$LiLaB_2O_5$	$TbCl_3$	0.05	2h-800	542 + 550	3.6	15	
$LiLB_2$-Tb-5	$LiLaB_2O_5$	$TbCl_3$	0.05	2h-800	542 + 550	3.0	20	
$LiIB_2$-Tb-5	$LiInB_2O_5$	$TbCl_3$	0.05	2h-800	542 + 550	0.68	16	
$LiIB_2$-Tb-6	$LiInB_2O_5$	$TbCl_3$	0.05	2h-850	542 + 550	6.9	20	
$LiYB_2$-Tb-5	$LiYB_2O_5$	$TbCl_3$	0.05	2h-800	542 + 550	1.5	18	
$LiYB_2$-Tb-6	$LiYB_2O_5$	$TbCl_3$	0.05	2h-850	542 + 550	5.8	21	
Z_2S-Mn-5-2	Zn_2SiO_4	Mn	10^{-4}	2h-1250	523	3.6	10	
Z_2S-Mn-6-1	Zn_2SiO_4	Mn	10^{-5}		523	1.1	8	
Z_2S-Mn-6-2	Zn_2SiO_4	Mn	10^{-5}	2h-1250	522	0.27	5	
Z_2S-Mn-6-2a	Zn_2SiO_4	Mn	10^{-5}		522	0.32	6	
Z_2S-Mn-6-2b	Zn_2SiO_4	Mn	10^{-5}		520 + blue	0.10	5	Blue luminescence due to incomplete Mn activation.
Z_2S-Mn-6-3	Zn_2SiO_4	Mn	10^{-5}	2h-1250	520	0.43	6	
Z_2S-Mn-7	Zn_2SiO_4	Mn	2×10^{-5}	2h-1250	528	0.95	7	Intensity increase after each exposure to CR.
Z_2S-Mn-7-a	Zn_2SiO_4	Mn	5×10^{-5}	2h-1250	523	0.79	8	

APPENDIX A (Continued)

Number	Composition	Activator and Concentration		Firing Time-Temp	Peak Wavelength (nm)	Intensity $1\,\mu a/cm^2$	Intensity Ratio	Comments
Z_2S-Mn-7-b	Zn_2SiO_4	Mn	$5x10^{-5}$	4h-1250	523	0.35	6	
Z_2S-Mn-8	Zn_2SiO_4	Mn	$5x10^{-5}$	2h-1250	520	1.35	10	
Z_2S-Mn-8-4	Zn_2SiO_4	Mn	$5x10^{-5}$	2h-1250	522	0.11	8	) Blue luminescence due to) incomplete activation by) Mn.
Z_2S-Mn-9	Zn_2SiO_4	Mn	$5x10^{-5}$	2h-1250	522	0.135	6	
Z_3P_2-Mn-1	$Zn_3(PO_4)_2$	Mn	10^{-5}	2h-950	550			Green luminescence due to incomplete Mn activation.
Z_3P_2-Mn-2	$Zn_3(PO_4)_2$	Mn	10^{-4}	4h-950	630	3.5	15	Double fired 2h-950 each.
Z_3P_2-Mn-3	$Zn_3(PO_4)_2$ +.02 Cd	Mn	10^{-4}	4h-950	631	0.2	9	Double fired 2h-950 each.
Z_3P_2-Mn-4	$Zn_3(PO_4)_2$ +.05 Cd	Mn	10^{-5}	2h-950	630	1.25	19	
Z_3P_2-Mn-5	$Zn_3(PO_4)_2$ +.05 Cd	Mn	$5x10^{-4}$	2h-950	630	1.5	16	
Z_3P_2-Mn-6	$Zn_3(PO_4)_2$ +.05 Cd	Mn	$5x10^{-4}$	2h-950	630	1.3	15	Also contains 7.5 ppm Ni.

APPENDIX B

Single Phosphor Screen Data

I Green Sulfide Compositions

Screen No.	Sample	Intensity at 1 $\mu a/cm^2$	Int. Ratio	Chromaticity Coordinates at 1.0 $\mu a/cm^2$ x	y	Comments
89a	ZC44-2C	1.3	65	0.273	0.504	
93a	ZC49	7.5	51	0.368	0.562	
22b-1	ZC48-2	3.9	118	0.345	0.574	
23b-1	ZC50	42.0	18	0.357	0.582	All exhibit a shift of chromaticity coordinates and the peak emission to larger values as current density is increased.
24b-2	ZC51	13.0	66	0.345	0.584	
25b-1	ZC52	1.3	118	0.330	0.565	
26b-2	ZC53	0.17	80	0.299	0.501	
27b-1	ZC54	1.05	130	0.350	0.559	
28b-1	ZC55	5.1	80	0.342	0.577	
91-a	ZC15-4	8.2	74			Reference Phosphor

APPENDIX B (Continued)

II Red Sulfide Compositions

Screen No.	Sample	Intensity at 1 $\mu a/cm^2$	Int. Ratio	Chromaticity Coordinates at 1.0 $\mu a/cm^2$ x	y	Comments
61a	CZ39-2	0.38	27	0.593	0.400	
62a	CZ61-1 & 7	0.8	61			
63a	CZ61-8	3.4	48	0.610	0.386	
65a	CZ67	0.96	25			
83a	CZ62	1.5	23			
84a	CZ63	1.0	21			
85a	CZ66	0.85	20	0.661	0.335	
86a	CZ67	1.3	22	0.659	0.335	
96a	CZAgNi-2	0.30	27			
16b	CZ87	1.2	120	0.577	0.417	
17b	CZ88	1.05	116	0.586	0.409	
18b	CZ89	1.25	83	0.588	0.408	
19b	CZ90	1.2	100	0.582	0.403	
20b	CZ91	0.71	83	0.582	0.412	
21b	CZ92	1.08	72	0.597	0.398	
31b	CZ64	3.8	24			
32b	CZ65	4.8	25			

APPENDIX B (Continued)

III Oxide Based Phosphors

Screen No.	Sample	Intensity at 1 $\mu a/cm^2$	Int. Ratio	Chromaticity Coordinates at 1.0 $\mu a/cm^2$ x	y	Comments
82a	Z_2SMn-8	0.74	11	0.193	0.717	Used in tube O-1
9b	$LI \cdot LB_4Tb$-2	1.45	15	0.326	0.573	
1b	$Z \cdot {}_3P_2Mn$-4	1.7	16			
13b	Z_3P_2Mn-5	2.05	13			
14b	Z_3P_2Mn-6	2.40	14			

APPENDIX B (Continued)

IV Color Shift of Green Phosphor Screens With Current Density

Screen No.	Sample	Chromaticity Coordinates at 0.1 $\mu a/cm^2$ x	y	1.0 $\mu a/cm^2$ x	y	10.0 $\mu a/cm^2$ x	y
25b-1	ZC52	0,310	0.524	0.330	0.565	0.336	0.577
26b-2	ZC53	(0.277)*	(0.434)*	0.299	0.501	0.325	0.554
27b-1	ZC54	0.324	0.517	0.350	0.559	0.354	0.569
28b-1	ZC55	0.322	0.562	0.342	0.577	0.340	0.585
22b	ZC48-2	0.334	0.552	0.345	0.574	0.344	0.581

* At 0.05 $\mu a/cm^2$

V Composition of Two Color Screens

Number	Composition	Screen Weight Ratio
45a	ZC12C (G) + CZ66 (R)	3/2
46a	ZC12C (G) + CZ66 (R)	1/1
47a	ZC12C (G) + CZ66 (R)	2/3
48a	ZC12C (G) + CZ67 (R)	3/2
49a	ZC12C (G) + CZ67 (R)	1/1
50a	ZC12C (G) + CZ67 (R)	2/3
51a	ZC12C (G) + LiI · Eμ68 (R)	3/2
52a	ZC12C (G) + LiI · Eμ68 (R)	1/1
53a	ZC12C (G) + LiI · Eμ68 (R)	2/3
71a	ZC44-2C (G) + CZ66 (R)	2/3
72a	ZC44-2C (G) + CZ66 (R)	1/1
73a	ZC44-2C (G) + CZ66 (R)	3/2
74a	CZ61-1 & 7 (R) + Z_2S-Mn-8	2/1
75a	CZ61-1 & 7 (R) + Z_2S-Mn-8	11/4
76a	CZ61-1 & 7 (R) + Z_2S-Mn-8	4/1
79a	ZC44-2C (G) + CZ66 (R)	2/1
80a	ZC44-2C (G) + CZ66 (R)	4/1
81a	CZ61-1 & 7 (R) + Z_2S-Mn-8 (G)	13/2
98a	ZC15-4 (G) + CZ67 (R)	2/3
99a	ZC15-4 (G) + CZ67 (R)	1/1

APPENDIX B (Continued)

V Composition of Two Color Screens

Number	Composition	Screen Weight Ratio
100a	ZC15-4 (G) + CZ67 (R)	3/2
3b	ZC48 (G) + CZ67 (R)	2/1
4b	ZC48 (G) + CZ67 (R)	1/2
7b	CZ61-1 & 7 (R) + Z_2S-MN-8 (G) + $LiLB_4$· Tb-2 (G)	25/3/2
8b	CZ61-1 & 7 (R) + Z_2S-Mn-8 (G) + $LiLB_4$· Tb-2 (G)	25/2/3
11b	ZC48 (G) + CZ63 (R)	1/2
12b	ZC48 (G) + CZ63 (R)	1/1
33b	ZC48 (G) + Z_3P_2-Mn-6 (R)	1/1
34b	ZC48 (G) + Z_3P_2-Mn-6 (R)	2/1
35b	ZC52 (G) + Z_3P_2-Mn-6 (R)	2/1
36b	ZC48 (G) + Z_3P_2-Mn-5 (R)	5/7

APPENDIX B (Continued)

VI Two Color Phosphor Screen Data

CIE Chromaticity Coordinates

Beam Current Density ($\mu a/cm^2$)

Screen No.	0.05		0.1		0.5		1.0		5.0		10.0	
	x	y	x	y	x	y	x	y	x	y	x	y
45a	--	--	0.504	0.448	0.449	0.503	0.424	0.527	--	--	0.393	0.552
46a	--	--	0.563	0.403	0.489	0.475	0.478	0.486	--	--	0.410	0.542
47a	--	--			0.530	0.441	0.495	0.473	--	--	0.464	0.500
48a	--	--	0.509	0.436	0.442	0.507	0.419	0.528	--	--	0.386	0.558
49a	--	--			0.503	0.461	0.474	0.488	--	--	0.416	0.537
50a	--	--	0.535	0.433	0.494	0.473	0.485	0.482	--	--	0.459	0.505
51a	--	--	0.403	0.464	0.355	0.532	0.343	0.550	--	--	0.322	0.570
52a	--	--	0.420	0.462	0.366	0.525	0.354	0.540	--	--	0.327	0.564
53a	--	--	0.454	0.424	0.400	0.503	0.375	0.537	--	--	0.343	0.560
71a	0.623	0.349	0.620	0.355	0.588	0.377	0.574	0.391	0.530	0.424	0.521	0.433
72a	0.602	0.356	0.594	0.362	0.566	0.386	0.543	0.408	0.503	0.442	0.492	0.454
73a	0.582	0.364	0.565	0.374	0.547	0.397	0.510	0.419	0.476	0.455	0.466	0.469
74a	0.256	0.668	0.271	0.655	0.350	0.593	0.395	0.559	--	--	0.462	0.505
75a	0.285	0.644	0.309	0.627	0.401	0.555	0.449	0.517	0.522	0.459	--	--
76a	0.325	0.612	0.354	0.592	0.462	0.506	0.506	0.471	0.562	0.425	0.567	0.423

APPENDIX B (Continued)

VI Two Color Phosphor Screen Data (Continued)

CIE Chromaticity Coordinates

Beam Current Density ($\mu a/cm^2$)

Screen No.	0.05		0.1		0.5		1.0		5.0		10.0	
	x	y	x	y	x	y	x	y	x	y	x	y
79a	0.575	0.360	--	--	0.464	0.456	0.447	0.469	0.426	0.495	0.433	0.500
80a	0.478	0.380	0.463	0.393	--	--	0.415	0.457	--	--	0.376	0.509
81a	0.337	0.608	0.363	0.587	0.464	0.503	0.506	0.471	0.555	0.433	0.564	0.426
98a	0.526	0.446	0.514	0.458	0.467	0.503	0.452	0.516	0.425	0.541	0.418	0.546
99a	0.488	0.474	0.473	0.488	0.436	0.526	0.426	0.535	0.402	0.557	0.399	0.560
100a	0.457	0.498	0.444	0.511	0.415	0.541	0.405	0.552	0.388	0.567	0.384	0.571
3b	0.587	0.392	0.574	0.406	0.526	0.449	0.504	0.469	0.472	0.498	0.460	0.509
4b	0.626	0.362	0.621	0.367	0.584	0.401	0.570	0.413	0.535	0.446	0.524	0.455
7b	0.416	0.537	0.441	0.518	0.518	0.459	0.544	0.440	0.570	0.420	0.569	0.421
8b	0.424	0.526	0.449	0.509	0.524	0.453	0.542	0.434	0.567	0.422	0.568	0.421
11b	0.604	0.378	0.593	0.390	0.544	0.434	0.521	0.454	0.484	0.486	0.469	0.499
12b	0.571	0.402	0.557	0.417	0.502	0.466	0.479	0.486	0.437	0.523	0.428	0.531
33b	0.587	0.382	0.568	0.398	0.492	0.461	0.462	0.486	0.411	0.527	0.403	0.534
34b	0.538	0.412	0.513	0.435	0.440	0.501	0.415	0.523	0.384	0.551	0.373	0.560
35b	0.603	0.360	0.595	0.367	0.540	0.409	0.505	0.437	0.426	0.505	0.406	0.523
36b	0.588	0.383	0.567	0.396	0.484	0.464	0.454	0.489	0.410	0.524	0.408	0.525

APPENDIX C

5-Inch CRT Data

All tubes except Q-1 were shipped to NASA as quarterly tubes representing the current status of development.

5-Inch Tube Data

No.	Composition Super/Subl.	Weight Ratio Super/ Subl.	Chromaticity Coordinated at 0.05 $\mu a/cm^2$ x	y	0.10 $\mu a/cm^2$ x	y	0.5 $\mu a/cm^2$ x	y	1.0 $\mu a/cm^2$ x	y	5.0 $\mu a/cm^2$ x	y	10.0 $\mu a/cm^2$ x	y
[1]K-1	CZ39-2 (R) $Z_2S \cdot$ Mn-6	7/3	0.251	0.659	0.284	0.644	0.354	0.588	0.408	0.545	0.486	0.484	0.505	0.469
*[2]M1-a	ZCDS341b + ZCDS35-1b (G) CZ66 (R)	3/2	0.581 (at 0.01 $\mu a/cm^2$)	0.360	0.585	0.363	0.555	0.383	0.538	0.393	0.494	0.318	0.477	0.423
*M1-b	CZ61-1 & 7 (R) $Z_2S \cdot$ Mn-5 (G)	3/1	0.224 (at 0.01 $\mu a/cm^2$)	0.697	0.251	0.675	0.314	0.625	0.372	0.579	0.462	0.507	0.477	0.496
[3]O-1	CZ61-1 & 7 (R) $Z_2S \cdot$ Mn-8 (G)	5/1	0.336	0.606	0.364	0.583	0.440	0.525	0.496	0.480	0.565	0.424	0.567	0.423
Q-1	ZC48 (G) Z_3P_2Mn-5 (R)	5/7	0.600	0.373	0.579	0.389	0.502	0.451	0.464	0.481	0.406	0.529	0.387	0.546
[4]Q-2	ZC48 (G) Z_3P_2Mn-5 (R)	5/7	0.597	0.376	0.577	0.391	0.495	0.455	0.449	0.495	0.404	0.526	0.391	0.548

* Split Screen Tube
1 5th Quarterly Tube
2 6th Quarterly Tube
3 7th Quarterly Tube
4 8th Quarterly Tube

Relative Brightness of Tube Q-2

Current Density $\mu a/cm^2$	Brightness (ft. l.)
0.05	0.9
0.10	1.6
0.50	10.0
1.0	23.0
5.0	190.0
10.0	400.0

NASA-Langley, 1970 — 9 CR-1514